

Multicomponent polymer flooding in two dimensional oil reservoir simulation

Sudarshan Kumar K^{*}, Praveen C[†] and G. D Veerappa Gowda[‡]

Abstract

We propose a high resolution finite volume scheme for a $(m+1) \times (m+1)$ system of nonstrictly hyperbolic conservation laws which models multicomponent polymer flooding in enhanced oil-recovery process in two dimensions. In the presence of gravity the flux functions need not be monotone and hence the exact Riemann problem is complicated and computationally expensive. To overcome this difficulty, we use the idea of discontinuous flux to reduce the coupled system into uncoupled system of scalar conservation laws with discontinuous coefficients. High order accurate scheme is constructed by introducing slope limiter in space variable and a strong stability preserving Runge-Kutta scheme in the time variable. The performance of the numerical scheme is presented in various situations by choosing a heavily heterogeneous hard rock type medium. Also the significance of dissolving multiple polymers in aqueous phase is presented.

1 Introduction

Simulation of two phase flow in porous media plays a key role in many engineering areas such as oil-recovery [5, 7, 35], environmental remediation [6] and water management in polymer electrolyte fuels cells [15]. We are interested in multi dimensional simulation of two phase flow in heterogeneous porous media arising in enhanced oil-recovery. It involves simultaneous flow of two immiscible phases (the aqueous phase and the oil phase) in a heterogeneous porous medium. We have assumed that m chemical components are dissolved in the aqueous phase. These components could, for example, be different polymers that all have different influence on the flow properties. We propose a high order finite volume scheme for the numerical simulation of Buckley-Leverett model with multicomponent polymer flooding by using the idea of discontinuous numerical flux developed in [4, 3]. For simplicity we let $\Omega = [0, 1] \times [0, 1]$ denote the two dimensional reservoir. Let $s \in [0, 1]$ denote the saturation of aqueous phase and $c = (c_1, c_2, \dots, c_m) \in [0, c_0]^m$ denote the concentration of the polymers dissolved in the aqueous phase, where c_0 is some non negative real number. Then in the absence of capillary pressure the governing equations form a $(m+1) \times (m+1)$ system of hyperbolic conservation laws [24, 25] given by

$$\begin{aligned} s_t + \nabla \cdot F(s, c_1, c_2, \dots, c_m, x) &= 0 \\ (s c_l + a_l(c_l))_t + \nabla \cdot (c_l F(s, c_1, c_2, \dots, c_m, x)) &= 0, \quad l = 1, 2, \dots, m \end{aligned} \quad (1)$$

where $(x, t) \in \Omega \times (0, \infty)$, $a_l : [0, 1] \rightarrow \mathbb{R}$ are given smooth functions and the flux $F : [0, 1] \times [0, c_0]^m \times \Omega \rightarrow \mathbb{R}^2$ is given by $F = (F_1, F_2)$,

$$F_1(s, c, x) = v_1(x) f(s, c), \quad f(s, c) = \frac{\lambda_w(s, c)}{\lambda_w(s, c) + \lambda_o(s)} \quad (2)$$

^{*}TIFR Centre for Applicable Mathematics Bangalore, sudarshan@math.tifrbng.res.in

[†]TIFR Centre for Applicable Mathematics Bangalore, praveen@math.tifrbng.res.in

[‡]TIFR Centre for Applicable Mathematics Bangalore, gowda@math.tifrbng.res.in

$$F_2(s, c, x) = [v_2(x) - (\rho_w - \rho_o)g\lambda_o(s, c)K(x)]f(s, c). \quad (3)$$

Here ρ_w, ρ_o are the densities of water and oil, g is the acceleration due to gravity. The quantities λ_w and λ_o are the mobilities of the water and oil phase respectively and $v = (v_1, v_2) \in \mathbb{R}^2$ is the total velocity given by Darcy law [16].

$$v = - \left((\lambda_w + \lambda_o)K(x) \frac{\partial p}{\partial x_1}, (\lambda_w + \lambda_o)K(x) \frac{\partial p}{\partial x_2} + (\lambda_w \rho_w + \lambda_o \rho_o)gK(x) \right) \quad (4)$$

where $K : \Omega \rightarrow [0, \infty)$ is the permeability of the rock which can be discontinuous in x and $p : \Omega \rightarrow \mathbb{R}$ is the pressure. If we assume incompressibility of the flow and if there are no sources, then the velocity is governed by

$$\nabla \cdot v = 0 \quad \text{in } \Omega \quad (5)$$

with some suitable boundary conditions for pressure on $\partial\Omega$. For instance in the inlet part of the boundary, water is pumped in at high pressure $p = p_I$ while a lower pressure $p = p_O$ is maintained on outlet, see Fig.14. On the remaining part of the boundary, the normal velocity is set to zero, which gives a Neumann boundary condition on pressure. Equations (1) and (5) form a system of coupled algebraic-differential equations and there is no time derivative involved in equation (5). A commonly used model for the mobilities are

$$\lambda_w(s, c) = \frac{s^2}{\mu_w(c)}, \quad \lambda_o(s) = \frac{(1-s)^2}{\mu_o} \quad (6)$$

where μ_w, μ_o are the viscosities of water and oil and $\mu_w = \mu_w(c)$ which is increasing in each of its variable c_i . The term a_l in (1) models the adsorption of the component l on the porous medium.

In the absence of polymer flooding or equivalently if the flux function is independent of c , then this problem (1) reduces to scalar equation. In [27] by using a fast marching method and in [29] by using semi-Godunov scheme method the problem is studied in the absence of polymer. Also in [17] two-phase flow problems are studied by using gradient schemes. It is well known that in the heterogeneous media, that is when the permeability $K(x)$ is discontinuous, fingering instability [12] will develop and which results in an inefficient oil-recovery. For example see Fig.17(a). As the concentration c increases, viscosity of water increases and the fingering effects reduces which leads to an efficient oil-recovery see Fig.17(b). In the presence of the concentration c the system (1) becomes coupled and non-strictly hyperbolic. When the concentration c is smooth, existence and uniqueness theory is established in [37] but we deal here with the case when c need not be smooth. For this system, developing a Godunov type upwind schemes are difficult as it needs a solution of Riemann problems. Most often numerical methods requires the calculation of eigenvalues and eigenvectors of the Jacobian matrix of the system. Here by using the idea of discontinuous flux we reduce the system to an uncoupled scalar equations with discontinuous coefficients. Next we study each scalar equation by using the idea of discontinuous flux. This approach does not require detailed information about the eigenstructure of the full system. Also in [29], the idea of discontinuous flux is used to study a coupled system arising in three-phase flows in porous media and shown its successfulness. Scalar conservation laws with discontinuous flux have been studied by many authors [2, 9, 10, 11, 13, 14, 18, 22, 26, 32]. In particular, in [3] a Godunov type finite volume scheme is proposed and convergence to a proper entropy solution is proved, provided the flux functions satisfies certain conditions like in §2. In one dimensional case for a (2×2) system this problem was studied in [4] and there proposed a finite volume scheme and named numerical flux as DFLU. This DFLU flux works even in cases where the upstream mobility gives an entropy violating solution [34]. Here we are extending DFLU to a multi dimensional case with high order accuracy. The difficulties of developing an upwind type numerical schemes in a highly heterogeneous media in the presence of gravity attracts the importance of the proposed work.

The paper is organized as follows. From §2 the idea of discontinuous flux for one dimensional problem is briefly explained and also numerical experiments for high order schemes are performed to show their efficiency. In §3 two dimensional problem is introduced and the idea of the one dimensional discontinuous flux is extended. Also high order accurate scheme is constructed by introducing slope limiter in space variable and a strong stability preserving Runge-Kutta scheme in the time variable [21]. The resulting schemes are shown to respect a maximum principle. Also two dimensional numerical results in various situation are shown for a quarter five-spot geometry.

2 System of equations in one dimension

The corresponding $(m+1) \times (m+1)$ system of equations in one-dimension in the presence of gravity is given by

$$\begin{aligned} s_t + \frac{\partial}{\partial x} F(s, c_1, c_2, \dots, c_m, x) &= 0 \\ (sc_l + a_l(c_l))_t + \frac{\partial}{\partial x} c_l F(s, c_1, c_2, \dots, c_m, x) &= 0, \quad l = 1, 2, \dots, m \end{aligned} \quad (7)$$

where $t > 0$ and $x \in \mathbb{R}$, $(s, c_1, c_2, \dots, c_m) = (s, c) \in [0, 1] \times [0, c_0]^m$ and

$$F(s, c, x) = [v - (\rho_w - \rho_o)g\lambda_o(s, c)K(x)]f(s, c). \quad (8)$$

In one dimension the solution v of the equation (5) reduces to a constant. We assume that the flux function satisfies following conditions:

1. $F(0, c_1, c_2, \dots, c_m, x) = 0$, $F(1, c_1, c_2, \dots, c_m, x) = v \forall x, c_l, \quad l = 1, 2, \dots, m$
2. The function $s \rightarrow F(s, c_1, c_2, \dots, c_m, x)$ is of convex type i.e, has no local maximum in the interior of $[0, 1] \times [0, c_0]^m$ see Fig.1
3. The adsorption term $a_l = a_l(c_l)$ satisfies $h_l(c_l) = \frac{da_l}{dc_l}(c_l) > 0, \forall c_l \in [0, 1]$.

The case when $v = 0$ and F does not change sign is studied in [4]. Here we assume v need not be zero and allow F to change sign, see Fig. 1. In the absence of gravity, $F_s = v f_s$ is non-negative or non-positive depending on $v \geq 0$ or $v \leq 0$. Hence F is increasing or decreasing in s accordingly. In the presence of gravity F_s becomes,

$$F_s = \frac{2s(1-s)}{\mu_w \mu_o (\lambda_w + \lambda_o)^2} [v + (\rho_w - \rho_o)gK(x)(s\lambda_w - (1-s)\lambda_o)]$$

which vanishes at $s = 0, 1$. Depending on the values of v, ρ_w, ρ_o, g, K , there can be a root $s_* \in (0, 1)$ which makes F non-monotone in s , as shown in Fig.1. If such a root exists, it is a root of the following cubic equation

$$r(c)s^3 - (1-s)^3 + z = 0, \quad r(c) = \frac{\mu_o}{\mu_w(c)}, \quad z = \frac{v\mu_o}{(\rho_w - \rho_o)gK}.$$

This cubic equation has one real and two complex roots, the real root is given by

$$s_* = \frac{1}{1+r} \left[1 - \frac{3\sqrt[3]{2}r}{(\alpha + \sqrt{\beta})^{1/3}} + \frac{1}{3\sqrt[3]{2}} (\alpha + \sqrt{\beta})^{1/3} \right]$$

where

$$\alpha = -27r + 27r^2 - 27z - 54rz - 27r^2z, \quad \beta = 2916r^3 + \alpha^2.$$

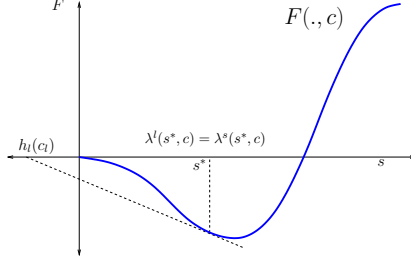


Figure 1: $\lambda^l = \lambda^s$

Since

$$F_{ss}(s_*, c, x) = \frac{6s_*(1-s_*)(\rho_w - \rho_o)gK(x)}{\mu_w\mu_o(\lambda_w + \lambda_o)^2} \left[\frac{s_*^2}{\mu_w} + \frac{(1-s_*)^2}{\mu_o} \right]$$

then F attains the maximum(minimum) at $s = s_*$ if $\rho_w > \rho_o$ ($\rho_w < \rho_o$). Note that the nature of the extremum depends only on the densities and is independent of the polymer concentrations c_l and the permeability K .

If $F(s, c, x) = F(s, c)$ then the system (7) can be put in the matrix form as

$$U_t + A(U)U_x = 0, \quad U = [s \ c_1 \ c_2 \ \dots \ c_m]^\top,$$

where $A(U)$ is the $(m+1) \times (m+1)$ Jacobian matrix

$$A(U) = \begin{pmatrix} \frac{\partial F}{\partial s} & \frac{\partial F}{\partial c_1} & \frac{\partial F}{\partial c_2} & \dots & \dots & \frac{\partial F}{\partial c_m} \\ 0 & \frac{F}{s+h_1} & 0 & \dots & \dots & 0 \\ 0 & 0 & \frac{F}{s+h_2} & 0 & \dots & 0 \\ \vdots & & \ddots & \ddots & & \vdots \\ \vdots & & \ddots & \ddots & & \vdots \\ 0 & \dots & \dots & \dots & 0 & \frac{F}{s+h_m} \end{pmatrix}$$

The eigenvalues of this system are given by

$$\lambda^s = \lambda(s, c) = \frac{\partial F}{\partial s}(s, c)$$

$$\lambda^l = \lambda^l(s, c) = \frac{F(s, c)}{s + h_l(c_l)}, \quad l = 1, 2, \dots, m.$$

We can observe that for any $c = (c_1, c_2, \dots, c_m) \in [0, 1] \times [0, c_0]^m$ and for some $l \in \{1, 2, \dots, m\}$ there exist at least one point $s^* = s^*(c) \in [0, 1]$ such that (see Fig.1).

$$\lambda^l(s^*, c) = \lambda^s(s^*, c).$$

For this couple (s^*, c) , $\lambda^l = \lambda^s$, hence eigenvalues may coincide and the problem is non strictly hyperbolic. The Rankine-Hugoniot condition corresponding to (7) is given by

$$\begin{aligned} F(s^R, c^R, x^+) - F(s^L, c^L, x^-) &= \sigma(s^R - s^L) \\ c_l^R F(s^R, c^R, x^+) - c_l^L F(s^L, c^L, x^-) &= \sigma(s^R c_l^R + a_l(c_l^R) - s^L c_l^L - a_l(c_l^L)) \end{aligned} \quad (9)$$

$\forall l = 1, 2, \dots, m.$

For details see [23, 25]. If $c^L = c^R$ (i.e. $c_l^L = c_l^R \quad \forall l = 1, 2, \dots, m$) then second equation reduces to the first equation of (9). This corresponds to the Rankine-Hugoniot condition for single Buckley-Leverett equation (1). Now we are interested in the case $c^L \neq c^R$, i.e. $c_l^L \neq c_l^R$ for some $l, 1 \leq l \leq m$. If we combine the two equations (9) then we may write

$$(c_l^R - c_l^L)F(s^L, c^L, x^-) = \sigma(c_l^R - c_l^L)s^L + \sigma(a_l(c_l^R) - a_l(c_l^L)) \quad (10)$$

Define the functions h_l^L by

$$h_l^L(c_l) = \begin{cases} \frac{a_l(c_l) - a_l(c_l^L)}{c_l - c_l^L} & \text{if } c_l \neq c_l^L, \\ h_l(c_l) & \text{if } c_l = c_l^L. \end{cases} \quad (11)$$

Now from (9) and (10), finally we get

$$\frac{F(s^R, c^R, x^+)}{s^R + \bar{h}} = \frac{F(s^L, c^L, x^-)}{s^L + \bar{h}} = \sigma, \quad (12)$$

where $\bar{h} = h_l^L(c_l^R) \quad (= h_l^L(c_l^R) \quad \forall l)$. Thus the Rankine-Hugoniot condition reduces to (12). This gives an idea how to obtain a weak solution of the Riemann problem to (7).

2.1 Riemann problem

For simplicity we restrict our study to the case when $m = 2$ in equation (7), i.e $c = (c_1, c_2)$. Also we assume that $F(s, c, x) = F(s, c)$. Consider the Riemann problem associated to the system (7) with the initial condition

$$s(x, 0) = \begin{cases} s_L & \text{if } x < 0, \\ s_R & \text{if } x > 0 \end{cases}, \quad c(x, 0) = \begin{cases} (c_1^L, c_2^L) & \text{if } x < 0, \\ (c_1^R, c_2^R) & \text{if } x > 0. \end{cases} \quad (13)$$

Solution to (7) and (13) is constructed by connecting states so that it should satisfies the Rankine-Hugoniot condition. There are two families of waves that arise in the solution of the Riemann problem referred to as s and c waves. s waves consists of rarefaction and shocks (or contact discontinuity) across which s changes continuously and discontinuously respectively, but across which both c_1 and c_2 remain constant. c waves consists solely of contact discontinuity across which both s and c_1, c_2 changes such that $\frac{F}{s+h}$ remains constant in the sense of (12). For different choices of c_L and c_R , the possible shapes of $F(s, c_L)$ and $F(s, c_R)$ are shown in Fig.2. We restrict to the case when $c_L > c_R$ (i.e., $c_l^L > c_l^R, l = 1, 2$). When $c_L > c_R$ the flux functions $s \rightarrow F(s, c^L)$ and $s \rightarrow F(s, c^R)$ are one of the shapes given in Fig.2. To explain the Riemann problem, for simplicity we consider the shape of the flux functions as in Fig.3

- Case 1: $s^L \leq s^*$
Draw a line through the points $(-\bar{h}, 0)$ and $(s^*, F(s^L, c_1^L, c_2^L))$. This intersects the curve $F(s, c_1^R, c_2^R)$ at the point \bar{s} , where $F_s(\bar{s}, c_1^R, c_2^R) \geq 0$. We divide this in two subcases.
- Case 1a: $s^R > \bar{s}$
 - (a) Connect (s^L, c_1^L, c_2^L) to (s^*, c_1^L, c_2^L) by a s -rarefaction wave (see Fig.3a).
 - (b) Connect (s^*, c_1^L, c_2^L) to (\bar{s}, c_1^R, c_2^R) by a c -wave with speed (see Fig.3a).

$$\sigma_c = \frac{F(\bar{s}, c_1^R, c_2^R)}{\bar{s} + \bar{h}} = F_s(s^*, c_1^L, c_2^L)$$

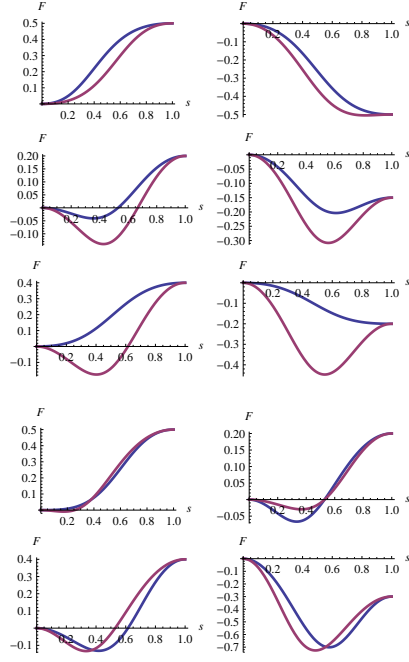


Figure 2: Possible shapes of flux functions for different choices of c_L and c_R .

(c) Connect (\bar{s}, c_1^R, c_2^R) to (s^R, c_1^R, c_2^R) by a s -rarefaction wave (see Fig.3a). For example if $F(s, c_1^L, c_2^L)$ and $F(s, c_1^R, c_2^R)$ are strictly convex functions then the corresponding solution of the Riemann problem is given by (see Fig.3b)

$$(s(x, t), c_1(x, t), c_2(x, t)) = \begin{cases} (s^L, c_1^L, c_2^L) & \text{if } x < \sigma_s t, \\ ((F_s)^{-1}(\frac{x}{t}, c_1^L, c_2^L), c_1^L, c_2^L) & \text{if } \sigma_s t < x < \sigma_c t, \\ (\bar{s}, c_1^R, c_2^R) & \text{if } \sigma_c t < x < \sigma_1 t, \\ ((F_s)^{-1}(\frac{x}{t}, c_1^R, c_2^R), c_1^R, c_2^R) & \text{if } \sigma_1 t < x < \sigma_2 t, \\ (s^R, c_1^R, c_2^R) & \text{if } x > \sigma_2 t. \end{cases}$$

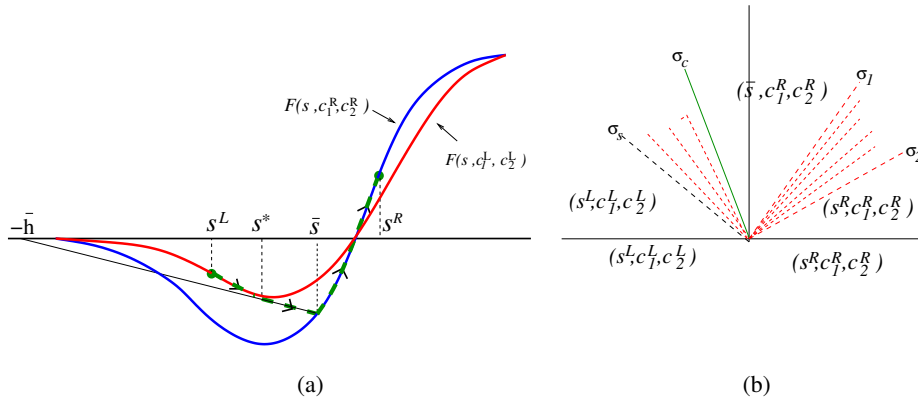


Figure 3: Solution of the Riemann problem (13) with $s^L \leq s^*$ and $s^R > \bar{s}$.

- Case 1b: $s^R \leq \bar{s}$

(a) Connect (s^L, c_1^L, c_2^L) to (s^*, c_1^L, c_2^L) by a s-rarefaction wave (see Fig.4a).

(b) Connect (s^*, c_1^L, c_2^L) to (\bar{s}, c_1^R, c_2^R) by a c-wave with speed (see Fig.4a).

$$\sigma_c = \frac{F(\bar{s}, c_1^R, c_2^R)}{\bar{s} + \bar{h}} = F_s(s^*, c_1^L, c_2^L)$$

(c) Connect (\bar{s}, c_1^R, c_2^R) to (s^R, c_1^R, c_2^R) by a s - shock wave with speed (see Fig.4a).

$$\sigma_s = \frac{F(\bar{s}, c_1^R, c_2^R) - F(s^R, c_1^R, c_2^R)}{\bar{s} - s^R}$$

In the case of convex fluxes we can write the solution of the Riemann problem as (see Fig.4b)

$$(s(x, t), c_1(x, t), c_2(x, t)) = \begin{cases} (s^L, c_1^L, c_2^L) & \text{if } x < \sigma_1 t, \\ ((F_s)^{-1}(\frac{x}{t}, c_1^L, c_2^L), c_1^L, c_2^L) & \text{if } \sigma_1 t < x < \sigma_c t, \\ (\bar{s}, c_1^R, c_2^R) & \text{if } \sigma_c t < x < \sigma_s t, \\ (s^R, c_1^R, c_2^R) & \text{if } x > \sigma_s t. \end{cases}$$

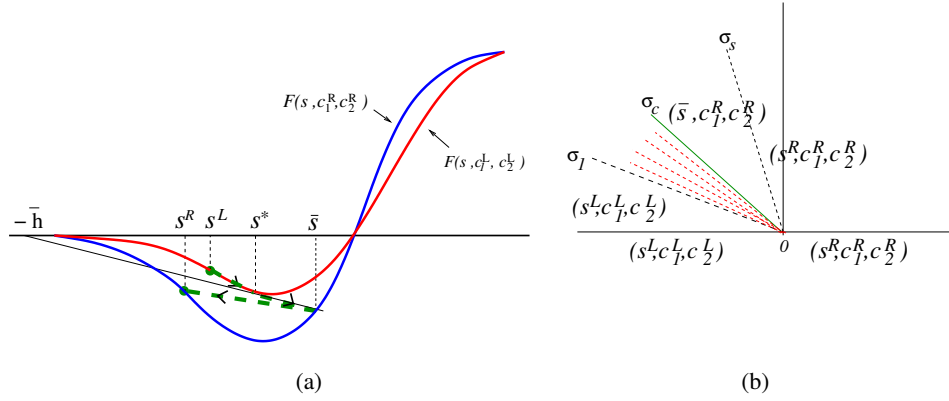


Figure 4: Solution of the Riemann problem (13) with $s^L \leq s^*$ and $s^R \leq \bar{s}$.

- Case 2: $s^L > s^*$

Draw a line joining the points $(-\bar{h}, 0)$ and $(s^L, F(s^L, c_1^L, c_2^L))$. Let (\bar{s}, c_1^R, c_2^R) be the point where this line meets the curve $F(s, c_1^R, c_2^R)$, where $F_s(\bar{s}, c_1^R, c_2^R) \geq 0$. Consider the following subcases.

- Case 2a: $s^R \geq \bar{s}$

(a) Connect (s^L, c_1^L, c_2^L) to (\bar{s}, c_1^R, c_2^R) by a c- shock wave with speed (see Fig.5a).

$$\sigma_c = \frac{F(s^L, c_1^L, c_2^L) - F(\bar{s}, c_1^R, c_2^R)}{s^L - \bar{s}}$$

(b) Connect (\bar{s}, c_1^R, c_2^R) to (s^R, c_1^R, c_2^R) by a s- rarefaction wave (see Fig.5a).

In the case of convex flux the solution of the Riemann problem is given by (see Fig.5b)

$$(s(x, t), c_1(x, t), c_2(x, t)) = \begin{cases} (s^L, c_1^L, c_2^L) & \text{if } x < \sigma_c t, \\ (\bar{s}, c_1^R, c_2^R) & \text{if } \sigma_c t < x < \sigma_1 t, \\ ((F_s)^{-1}(\frac{x}{t}, c_1^R, c_2^R), c_1^R, c_2^R) & \text{if } \sigma_1 t < x < \sigma_2 t, \\ (s^R, c_1^R, c_2^R) & \text{if } x > \sigma_2 t. \end{cases}$$

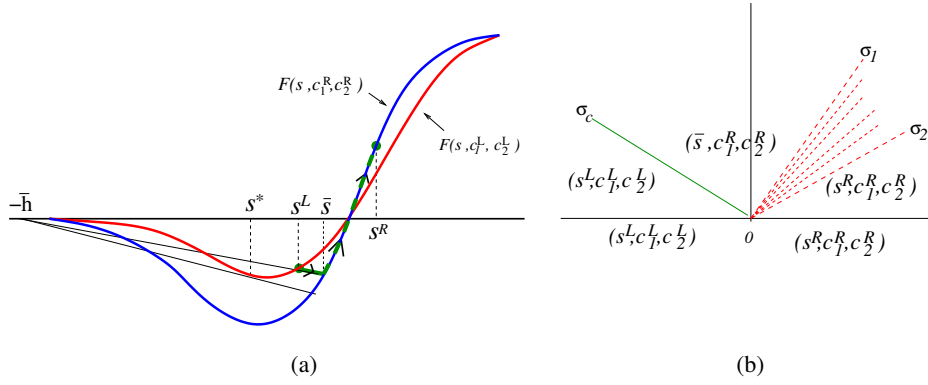


Figure 5: Solution of the Riemann problem (13) with $s^L > s^*$ and $s^R \geq \bar{s}$.

- Case 2b: $s^L < \bar{s}$

(a) Connect (s^L, c_1^L, c_2^L) to (\bar{s}, c_1^R, c_2^R) by a c -shock wave with speed (see Fig.6a).

$$\sigma_c = \frac{F(s^L, c_1^L, c_2^L) - F(\bar{s}, c_1^R, c_2^R)}{s^L - \bar{s}}$$

(b) Connect (\bar{s}, c_1^R, c_2^R) to (s^R, c_1^R, c_2^R) by a s -shock wave with speed (see Fig.6a).

$$\sigma_s = \frac{F(\bar{s}, c_1^R, c_2^R) - F(s^R, c_1^R, c_2^R)}{\bar{s} - s^R}$$

In the case of convex flux the solution of the Riemann problem is given by (see Fig.6b)

$$(s(x, t), c_1(x, t), c_2(x, t)) = \begin{cases} (s^L, c_1^L, c_2^L) & \text{if } x < \sigma_c t, \\ (\bar{s}, c_1^R, c_2^R) & \text{if } \sigma_c t < x < \sigma_s t, \\ (s^R, c_1^R, c_2^R) & \text{if } x > \sigma_s t. \end{cases}$$

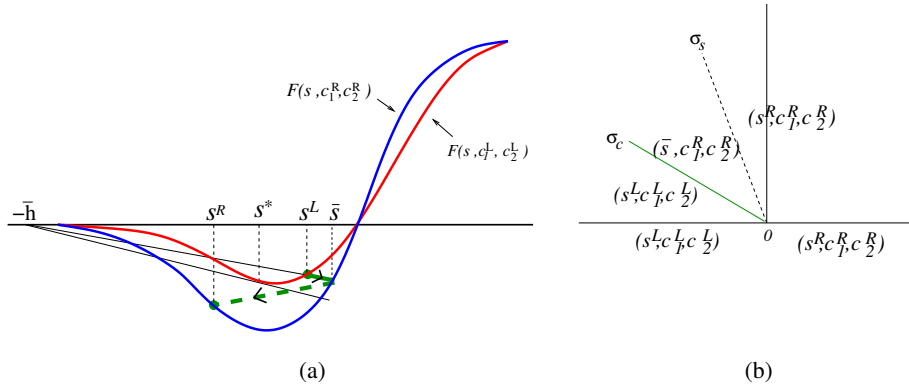


Figure 6: Solution of the Riemann problem (13) with $s^L > s^*$ and $s^R < \bar{s}$.

Remark: When the flux function $F(s, c, x)$ is smooth in s and c and discontinuous in the x variable then the construction of Riemann problem is explained in the appendix of [4]. Here also we can construct the solution of Riemann problem in a similar way.

2.2 Finite volume scheme

We define the space grid points as $x_{i+\frac{1}{2}} = ih$, $h > 0$ and $i \in \mathbb{Z}$ and for $\Delta t > 0$ define the time discretization points $t_n = n\Delta t$ for all non-negative integer n , and $\lambda = \frac{\Delta t}{h}$. The Finite volume scheme for the system (7) is given by

$$\begin{aligned} s_i^{n+1} &= s_i^n - \lambda(F_{i+\frac{1}{2}}^n - F_{i-\frac{1}{2}}^n) \\ c_{1i}^{n+1}s_i^{n+1} + a_1(c_{1i}^{n+1}) &= c_{1i}^n s_i^n + a_1(c_{1i}^n) - \lambda(G_{1i+\frac{1}{2}}^n - G_{1i-\frac{1}{2}}^n) \\ c_{2i}^{n+1}s_i^{n+1} + a_2(c_{2i}^{n+1}) &= c_{2i}^n s_i^n + a_2(c_{2i}^n) - \lambda(G_{2i+\frac{1}{2}}^n - G_{2i-\frac{1}{2}}^n). \end{aligned} \quad (14)$$

where the numerical flux $F_{i+\frac{1}{2}}^n$, $G_{1i+\frac{1}{2}}^n$ and $G_{2i+\frac{1}{2}}^n$ are associated with the flux functions $F(s, c, x)$ and $G_l(s, c, x) = c_l F(s, c, x)$, $l = 1, 2$ and are functions of the left and right values of the saturation s and the concentration c at $x_{i+\frac{1}{2}}$:

$$F_{i+\frac{1}{2}}^n = \bar{F}(s_i^n, c_{1i}^n, c_{2i}^n, s_{i+1}^n, c_{1i+1}^n, c_{2i+1}^n, x_{i+\frac{1}{2}}), \quad G_{l i+\frac{1}{2}}^n = \bar{G}_l(s_i^n, c_{1i}^n, c_{2i}^n, s_{i+1}^n, c_{1i+1}^n, c_{2i+1}^n, x_{i+\frac{1}{2}}).$$

The choice of the numerical flux functions \bar{F} and \bar{G}_l ($l = 1, 2$) determines the numerical scheme. Once we compute s_i^{n+1} from the first equation of (14) then we recover c_{1i}^{n+1} and c_{2i}^{n+1} from second and third equation respectively using an iterative method, like Newton-Raphson method.

Now we briefly explain the DFLU flux of [4] and Godunov flux.

2.3 The DFLU numerical flux

The DFLU flux is an extension of the Godunov scheme that was proposed and analyzed in [3] for scalar conservations laws with a flux function discontinuous in space. We define

$$G_{l i+\frac{1}{2}}^n = \begin{cases} c_{li}^n F_{i+\frac{1}{2}}^n & \text{if } F_{i+\frac{1}{2}}^n > 0 \\ c_{li+1}^n F_{i+\frac{1}{2}}^n & \text{if } F_{i+\frac{1}{2}}^n \leq 0 \end{cases} \quad l = 1, 2. \quad (15)$$

Now the choice of the numerical scheme depends on the choice of $F_{i+\frac{1}{2}}^n$. To do so we treat $c(x, t)$ in $F(s, c, x)$ as a known function which may be discontinuous at the space discretization points and F is allowed to be discontinuous in the x variable at the same space discretization points. Therefore on each rectangle $(x_{i-\frac{1}{2}}, x_{i+\frac{1}{2}}) \times (t_n, t_{n+1})$, we consider the conservation law:

$$s_t + F(s, c_{1i}^n, c_{2i}^n, x)_x = 0$$

with initial condition $s(x, 0) = s_i^n$ for $x_{i-\frac{1}{2}} < x < x_{i+\frac{1}{2}}$ (see Fig.7). The above problem can be

$t = t_{n+1}$		
	$s_t + F(s, c_{1i}^n, c_{2i}^n, x)_x = 0$	$s_t + F(s, c_{1i+1}^n, c_{2i+1}^n, x)_{x+1} = 0$
$t = t_n$	$s(t_n) = s_i^n$	$s(t_n) = s_{i+1}^n$
	$x_{i-\frac{1}{2}}$	$x_{i+\frac{1}{2}}$

Figure 7: The flux functions $F(\cdot, c_1, c_2, x)$ is discontinuous in c_1, c_2 and x at the discretization points.

considered as a conservation law with flux function discontinuous in x for which DFLU flux can be used. Then the DFLU flux is given as

$$\begin{aligned} F_{i+\frac{1}{2}}^n &= F^{DFLU}(s_i^n, c_{1i}^n, c_{2i}^n s_{i+1}^n, c_{1i+1}^n, c_{2i+1}^n) \\ &= \max\{F(\max\{s_i^n, \theta_i^n\}, c_{1i}^n, c_{2i}^n, x_i), F(\min\{s_{i+1}^n, \theta_{i+1}^n\}, c_{1i+1}^n, c_{2i+1}^n, x_{i+1})\}, \end{aligned}$$

where $\theta_i^n = \operatorname{argmin} F(\cdot, c_{1i}^n, c_{2i}^n, x_i)$.

2.4 The Godunov flux

The Godunov flux at the grid point $x_{i+\frac{1}{2}}$ is calculated by using the solution of the Riemann problem:

$$\begin{aligned} s_t + F(s, c, x)_x &= 0 \\ (sc_1 + a_1(c_1))_t + (c_1 F(s, c, x))_x &= 0 \\ (sc_2 + a_2(c_2))_t + (c_2 F(s, c, x))_x &= 0 \end{aligned} \tag{16}$$

in the domain $(x_{i-\frac{1}{2}}, x_{i+\frac{1}{2}}) \times (t_n, t_{n+1})$, with the initial condition

$$(s(x, t_n), c_1(x, t_n), c_2(x, t_n)) = \begin{cases} (s_i^n, c_{1i}^n, c_{2i}^n) & \text{if } x < x_{i+\frac{1}{2}} \\ (s_{i+1}^n, c_{1i+1}^n, c_{2i+1}^n) & \text{if } x > x_{i+\frac{1}{2}}. \end{cases}$$

The numerical fluxes are given by

$$F_{i+\frac{1}{2}}^n = F(s(x_{i+\frac{1}{2}}, t), c(x_{i+\frac{1}{2}}, t), x_{i+\frac{1}{2}}), \quad t_n < t < t_{n+1}$$

and

$$G_{l, i+\frac{1}{2}}^n = c_l(x_{i+\frac{1}{2}}, t) F_{i+\frac{1}{2}}^n, \quad l = 1, 2.$$

Remark: In general Godunov and DFLU flux may differ, for details see [4].

2.5 The Upstream Mobility flux

This flux is designed by petroleum engineers from physical consideration. It is an ad-hoc flux for two-phase flow in porous media which corresponds to the approximate solution to the Riemann problem [8]. To define the upstream mobility flux, assume that the absolute permeability $K(x) > 0$ and we redefine the flux function in (8) as

$$F(s, c, x) = \frac{K\lambda_w}{K\lambda_w + K\lambda_o} [v - (\rho_w - \rho_o)gK\lambda_o(s, c)] \tag{17}$$

Now if we take $\lambda_w = K\lambda_w$ and $\lambda_o = K\lambda_o$, the flux function becomes

$$F(s, c, x) = \frac{\lambda_w}{\lambda_w + \lambda_o} [v - (\rho_w - \rho_o)g\lambda_o(s, c)]$$

Now the numerical fluxes are given by

$$\begin{aligned} F_{i+\frac{1}{2}}^n(s_i^n, c_{1i}^n, c_{2i}^n, s_{i+1}^n, c_{1i+1}^n, c_{2i+1}^n) &= \frac{\lambda_w^*}{\lambda_w^* + \lambda_o^*} [v - (\rho_w - \rho_o)g\lambda_o^*], \\ \lambda_\ell^* &= \begin{cases} \lambda_\ell(s_i^n, c_{1i}^n, c_{2i}^n, K_i) & \text{if } v - (\rho_\ell - \rho_i)g\lambda_\ell > 0, \quad i = w, o, i \neq \ell, \\ \lambda_\ell(s_{i+1}^n, c_{1i+1}^n, c_{2i+1}^n, K_{i+1}) & \text{if } v - (\rho_\ell - \rho_i)g\lambda_\ell \leq 0, \quad i = w, o, i \neq \ell \end{cases} \end{aligned}$$

and $G_{l, i+\frac{1}{2}}^n$ ($l = 1, 2$) are given as in (15).

Remark: The Upstream mobility flux works only for the flux function which is of the form as in (17) where as DFLU flux can be applied for any flux function which satisfies the assumptions of §2.

2.6 High-order schemes

In order to develop the second order scheme, we follow the method of lines approach in which space and time discretization are performed separately. In the first step, spatial discretization using piecewise linear reconstruction is made which leads to a system of ODE which can be written as

$$\frac{dU}{dt} + R(U) = 0, \quad U = \begin{bmatrix} s \\ sc_1 + a_1(c_1) \\ sc_2 + a_2(c_2) \end{bmatrix}, \quad R(U)_i = \frac{1}{\Delta x} \begin{bmatrix} F_{i+\frac{1}{2}} - F_{i-\frac{1}{2}} \\ G_{1i+\frac{1}{2}} - G_{1i-\frac{1}{2}} \\ G_{2i+\frac{1}{2}} - G_{2i-\frac{1}{2}} \end{bmatrix} \quad (18)$$

The high order accurate fluxes are given by

$$F_{i+\frac{1}{2}} = F(s_{i+\frac{1}{2}}^L, s_{i+\frac{1}{2}}^R, c_{1i+\frac{1}{2}}^L, c_{2i+\frac{1}{2}}^L, c_{1i+\frac{1}{2}}^R, c_{2i+\frac{1}{2}}^R) \\ G_{li+\frac{1}{2}} = \begin{cases} c_{li+\frac{1}{2}}^L F_{i+\frac{1}{2}} & \text{if } F_{i+\frac{1}{2}} > 0 \\ c_{li+\frac{1}{2}}^R F_{i+\frac{1}{2}} & \text{if } F_{i+\frac{1}{2}} \leq 0 \end{cases} \quad l = 1, 2, \quad (19)$$

The quantities with superscripts L and R denote the reconstructed values of the variables to the left and right of the corresponding cell face. For any quantity u , we can define the reconstruction as follows:

$$u_{i+\frac{1}{2}}^L = u_i + \frac{1}{2}\delta_i, \quad u_{i+\frac{1}{2}}^R = u_{i+1} - \frac{1}{2}\delta_{i+1} \quad (20)$$

where

$$\delta_i = \min\left(\theta(u_i - u_{i-1}), \frac{1}{2}(u_{i+1} - u_{i-1}), \theta(u_{i+1} - u_i)\right), \quad \theta \in [1, 2]. \quad (21)$$

Finally the time integration of the ODE (18) must be high order accurate in order for the scheme to be high order accurate. A third order accurate, strong stability preserving Runge-Kutta scheme due to Shu-Osher is given by

$$\begin{aligned} V^{(0)} &= U^n \\ V^{(1)} &= V^{(0)} - \Delta t R(V^{(0)}) \\ V^{(2)} &= \frac{3}{4}U^n + \frac{1}{4}[V^{(1)} - \Delta t R(V^{(1)})] \\ V^{(3)} &= \frac{1}{3}U^n + \frac{2}{3}[V^{(2)} - \Delta t R(V^{(2)})] \\ U^{n+1} &= V^{(3)} \end{aligned}$$

If the explicit scheme (14) is stable in the norm $\|\cdot\|$, i.e., if

$$\Delta t \leq \Delta t_c \implies \|U - \Delta t R(U)\| \leq \|U\|, \quad \text{where } \Delta t_c \text{ is the CFL restricted time step,} \quad (22)$$

then the above Runge-Kutta scheme is also stable in the same norm under the same time-step restriction (cf.[20, 21]).

2.7 Maximum principle on saturation

Let us write

$$\bar{s}^n = (\bar{s}_i^n)_{i=1}^4 = (s_{i-\frac{1}{2}}^{nL}, s_{i-\frac{1}{2}}^{nR}, s_{i+\frac{1}{2}}^{nL}, s_{i+\frac{1}{2}}^{nR}) \\ \bar{c}^n = (\bar{c}_i^n)_{i=1}^8 = (c_{1i-\frac{1}{2}}^{nL}, c_{1i-\frac{1}{2}}^{nR}, c_{1i+\frac{1}{2}}^{nL}, c_{1i+\frac{1}{2}}^{nR}, c_{2i-\frac{1}{2}}^{nL}, c_{2i-\frac{1}{2}}^{nR}, c_{2i+\frac{1}{2}}^{nL}, c_{2i+\frac{1}{2}}^{nR})$$

The updated value of the saturation (14) can be written as

$$s_i^{n+1} = H(\bar{s}^n, \bar{c}^n).$$

Where H is Lipschitz continuous in saturation and concentration. Since the slope limiter preserves the average value of the solution in each cell, we can express this as

$$s_i^{n+1} = \frac{s_{i+\frac{1}{2}}^{nL} + s_{i-\frac{1}{2}}^{nR}}{2} - \lambda(F_{i+\frac{1}{2}}^n - F_{i-\frac{1}{2}}^n). \quad (23)$$

If we differentiate H with respect to its variables \bar{s}_i^n we can observe that $\frac{\partial}{\partial \bar{s}_i^n} H \geq 0$ provided

$$\lambda \left| \frac{\partial}{\partial \bar{s}_i^n} F_{i \pm \frac{1}{2}}^n \right| \leq \frac{1}{2}. \quad (24)$$

Let

$$M = \sup_s \left\{ \frac{\partial F_1}{\partial s}, \frac{\partial F_2}{\partial s}, \frac{F_1}{s + h_l}, \frac{F_2}{s + h_l} \right\},$$

then the condition (24) reduces to,

$$\lambda M \leq \frac{1}{2}. \quad (25)$$

This shows that H is monotone in each of its variable. Using these facts we have the following lemmas.

Lemma 2.1 *Let $s_0 \in [0, 1]$ be the initial data and let $\{s_i^n\}$ be the corresponding solution calculated by the finite volume scheme (14) using DFLU flux along with slope limiter. If the CFL given in (25) holds then*

$$0 \leq s_i^n \leq 1 \quad \forall, i \text{ and } n. \quad (26)$$

Proof: From the property of slope limiter we can observe that whenever $0 \leq s_i^n \leq 1$ then the reconstructed values satisfies

$$0 \leq s_{i \pm \frac{1}{2}}^{nL}, s_{i \pm \frac{1}{2}}^{nR} \leq 1 \quad \forall i \text{ and } n$$

Using this property and the monotonicity of the H , we get

$$0 = H(\mathbf{0}, \bar{c}^n) \leq H(\bar{s}^n, \bar{c}^n) = s_i^{n+1} \leq H(\mathbf{1}, \bar{c}^n) = 1$$

This proves that

$$0 \leq s_i^{n+1} \leq 1 \quad \forall i, n.$$

■

2.8 Maximum principle and TVD for concentration

Theorem 2.2 *Let $\{c_{1i}^n\}, \{c_{2i}^n\}$ be the solution calculated by the finite volume scheme (14) using DFLU flux with slope limiter. Under the CFL condition $\lambda M \leq \frac{1}{2}$, concentration $c = (c_1, c_2)$ satisfies*

$$(a) \quad \min\{c_{li-1}^n, c_{li}^n, c_{li+1}^n\} \leq c_{li}^{n+1} \leq \max\{c_{li-1}^n, c_{li}^n, c_{li+1}^n\} \quad \forall n \in \mathbb{Z}^+, i \in \mathbb{Z} \quad l = 1, 2.$$

$$(b) \quad \sum_i |c_{li}^{n+1} - c_{li-1}^{n+1}| \leq \sum_i |c_{li}^n - c_{li-1}^n| \quad \forall n \in \mathbb{Z}^+, \quad l = 1, 2.$$

Proof: From the finite volume scheme (14),

$$\begin{aligned} s_i^{n+1} &= s_i^n - \lambda(F_{i+\frac{1}{2}}^n - F_{i-\frac{1}{2}}^n) \\ c_{1i}^{n+1} s_i^{n+1} + a_1(c_{1i}^{n+1}) &= c_{1i}^n s_i^n + a_1(c_{1i}^n) - \lambda(G_{1i+\frac{1}{2}}^n - G_{1i-\frac{1}{2}}^n) \\ c_{2i}^{n+1} s_i^{n+1} + a_2(c_{2i}^{n+1}) &= c_{2i}^n s_i^n + a_2(c_{2i}^n) - \lambda(G_{2i+\frac{1}{2}}^n - G_{2i-\frac{1}{2}}^n). \end{aligned}$$

We can express the numerical flux $G_{1i+\frac{1}{2}}, G_{2i+\frac{1}{2}}$ as (here we suppress the index n for fluxes)

$$\begin{aligned} G_{1i+\frac{1}{2}} &= c_{1i+\frac{1}{2}}^L F_{i+\frac{1}{2}}^+ + c_{1i+\frac{1}{2}}^R F_{i+\frac{1}{2}}^- \\ G_{2i+\frac{1}{2}} &= c_{2i+\frac{1}{2}}^L F_{i+\frac{1}{2}}^+ + c_{2i+\frac{1}{2}}^R F_{i+\frac{1}{2}}^-, \end{aligned}$$

where

$$F_{i+\frac{1}{2}}^+ = \max\{F_{i+\frac{1}{2}}, 0\}, \quad F_{i+\frac{1}{2}}^- = \min\{F_{i+\frac{1}{2}}, 0\}$$

We write the scheme (14) as

$$s_i^{n+1} c_{1i}^{n+1} + a_l(c_{1i}^{n+1}) - s_i^n c_{1i}^n - a_l(c_{1i}^n) + \lambda(c_{1i+\frac{1}{2}}^{nL} F_{i+\frac{1}{2}}^+ + c_{1i+\frac{1}{2}}^{nR} F_{i+\frac{1}{2}}^- - (c_{1i-\frac{1}{2}}^{nL} F_{i-\frac{1}{2}}^+ + c_{1i-\frac{1}{2}}^{nR} F_{i-\frac{1}{2}}^-)) = 0$$

By adding and subtracting the term $s_i^{n+1} c_{1i}^n$, we get

$$\begin{aligned} (s_i^{n+1} + a_l'(\zeta_i^{n+\frac{1}{2}}))(c_{1i}^{n+1} - c_{1i}^n) + c_{1i}^n (s_i^{n+1} - s_i^n) \\ + \lambda(c_{1i+\frac{1}{2}}^{nL} F_{i+\frac{1}{2}}^+ + c_{1i+\frac{1}{2}}^{nR} F_{i+\frac{1}{2}}^- - (c_{1i-\frac{1}{2}}^{nL} F_{i-\frac{1}{2}}^+ + c_{1i-\frac{1}{2}}^{nR} F_{i-\frac{1}{2}}^-)) = 0. \end{aligned}$$

where $a_l(c_{1i}^{n+1}) - a_l(c_{1i}^n) = a_l'(\zeta_i^{n+\frac{1}{2}})(c_{1i}^{n+1} - c_{1i}^n)$, for some $\zeta_i^{n+\frac{1}{2}}$ between c_{1i}^{n+1} and c_{1i}^n . By replacing $s_i^{n+1} - s_i^n$ by $-\lambda(F_{i+\frac{1}{2}} - F_{i-\frac{1}{2}})$ and splitting $F_{i\pm\frac{1}{2}}$ by $(F_{i\pm\frac{1}{2}}^+ + F_{i\pm\frac{1}{2}}^-)$ we have

$$\begin{aligned} (s_i^{n+1} + a_l'(\zeta_i^{n+\frac{1}{2}}))(c_{1i}^{n+1} - c_{1i}^n) - \lambda c_{1i}^n (F_{i+\frac{1}{2}}^+ + F_{i+\frac{1}{2}}^- - F_{i-\frac{1}{2}}^+ - F_{i-\frac{1}{2}}^-) \\ + \lambda(c_{1i+\frac{1}{2}}^{nL} F_{i+\frac{1}{2}}^+ + c_{1i+\frac{1}{2}}^{nR} F_{i+\frac{1}{2}}^- - (c_{1i-\frac{1}{2}}^{nL} F_{i-\frac{1}{2}}^+ + c_{1i-\frac{1}{2}}^{nR} F_{i-\frac{1}{2}}^-)) = 0. \end{aligned}$$

By rearranging the terms in the above equation we get

$$\begin{aligned} (s_i^{n+1} + a_l'(\zeta_i^{n+\frac{1}{2}}))(c_{1i}^{n+1} - c_{1i}^n) + \lambda F_{i+\frac{1}{2}}^+ (c_{1i+\frac{1}{2}}^{nL} - c_{1i}^n) \\ + \lambda F_{i+\frac{1}{2}}^- (c_{1i+\frac{1}{2}}^{nR} - c_{1i}^n) + \lambda F_{i-\frac{1}{2}}^+ (c_{1i}^n - c_{1i-\frac{1}{2}}^{nL}) + \lambda F_{i-\frac{1}{2}}^- (c_{1i}^n - c_{1i-\frac{1}{2}}^{nR}) = 0. \end{aligned}$$

Note that

$$c_{1i+\frac{1}{2}}^{nL} = c_{1i}^n + \frac{\delta_i}{2}, \quad c_{1i-\frac{1}{2}}^{nR} = c_{1i}^n - \frac{\delta_i}{2},$$

and δ_i is the slope limiter given by

$$\delta_i = \min\left(\theta(c_{1i}^n - c_{1i-1}^n), \frac{1}{2}(c_{1i+1}^n - c_{1i-1}^n), \theta(c_{1i+1}^n - c_{1i}^n)\right).$$

After substituting the values for $c_{1i\pm\frac{1}{2}}^{nL}$ and $c_{1i\pm\frac{1}{2}}^{nR}$ the above equation becomes

$$\begin{aligned} (s_i^{n+1} + a_l'(\zeta_i^{n+\frac{1}{2}}))(c_{1i}^{n+1} - c_{1i}^n) + \lambda F_{i+\frac{1}{2}}^+ \frac{\delta_i}{2} + \lambda F_{i+\frac{1}{2}}^- \left(1 - \frac{\delta_{i+1}}{2(c_{1i+1}^n - c_{1i}^n)}\right) (c_{1i+1}^n - c_{1i}^n) \\ + \lambda F_{i-\frac{1}{2}}^+ \left(1 - \frac{\delta_{i-1}}{2(c_{1i}^n - c_{1i-1}^n)}\right) (c_{1i}^n - c_{1i-1}^n) + \lambda F_{i-\frac{1}{2}}^- \frac{\delta_i}{2} = 0. \end{aligned}$$

Now we can write

$$c_l^{n+1} = c_l^n - \lambda \frac{F_{i+\frac{1}{2}}^+}{2(s_i^{n+1} + a_l'(\zeta_i^{n+\frac{1}{2}}))(c_l^n - c_{l-1}^n)} \delta_i (c_l^n - c_{l-1}^n) \quad (27)$$

$$\begin{aligned} & - \lambda \frac{F_{i+\frac{1}{2}}^-}{(s_i^{n+1} + a_l'(\zeta_i^{n+\frac{1}{2}}))} \left(1 - \frac{\delta_{i+1}}{2(c_{l+1}^n - c_l^n)}\right) (c_{l+1}^n - c_l^n) \\ & - \lambda \frac{F_{i-\frac{1}{2}}^+}{(s_i^{n+1} + a_l'(\zeta_i^{n+\frac{1}{2}}))} \left(1 - \frac{\delta_{i-1}}{2(c_l^n - c_{l-1}^n)}\right) (c_l^n - c_{l-1}^n) \end{aligned} \quad (28)$$

$$\begin{aligned} & - \lambda \frac{F_{i-\frac{1}{2}}^-}{(s_i^{n+1} + a_l'(\zeta_i^{n+\frac{1}{2}}))} \frac{\delta_i}{2(c_{l+1}^n - c_l^n)} (c_{l+1}^n - c_l^n) \\ & = c_l^n - \alpha_{i-\frac{1}{2}}^1 (c_l^n - c_{l-1}^n) + \alpha_{i+\frac{1}{2}}^2 (c_{l+1}^n - c_l^n) - \alpha_{i-\frac{1}{2}}^3 (c_l^n - c_{l-1}^n) + \alpha_{i+\frac{1}{2}}^4 (c_{l+1}^n - c_l^n) \\ & = c_l^n - (\alpha_{i-\frac{1}{2}}^1 + \alpha_{i-\frac{1}{2}}^3) (c_l^n - c_{l-1}^n) + (\alpha_{i+\frac{1}{2}}^2 + \alpha_{i+\frac{1}{2}}^4) (c_{l+1}^n - c_l^n) \\ & = c_l^n - C_{i-\frac{1}{2}}^n (c_l^n - c_{l-1}^n) + D_{i+\frac{1}{2}}^n (c_{l+1}^n - c_l^n), \end{aligned} \quad (29)$$

where

$$C_{i-\frac{1}{2}}^n = \alpha_{i-\frac{1}{2}}^1 + \alpha_{i-\frac{1}{2}}^3, \quad D_{i+\frac{1}{2}}^n = \alpha_{i+\frac{1}{2}}^2 + \alpha_{i+\frac{1}{2}}^4$$

and

$$\begin{aligned} \alpha_{i-\frac{1}{2}}^1 &= \lambda \frac{F_{i+\frac{1}{2}}^+}{(s_i^{n+1} + a_l'(\zeta_i^{n+\frac{1}{2}}))2(c_l^n - c_{l-1}^n)} \delta_i, \quad \alpha_{i+\frac{1}{2}}^2 = -\lambda \frac{F_{i+\frac{1}{2}}^-}{(s_i^{n+1} + a_l'(\zeta_i^{n+\frac{1}{2}}))} \left(1 - \frac{\delta_{i+1}}{2(c_{l+1}^n - c_l^n)}\right) \\ \alpha_{i-\frac{1}{2}}^3 &= \lambda \frac{F_{i-\frac{1}{2}}^+}{(s_i^{n+1} + a_l'(\zeta_i^{n+\frac{1}{2}}))} \left(1 - \frac{\delta_{i-1}}{2(c_l^n - c_{l-1}^n)}\right), \quad \alpha_{i+\frac{1}{2}}^4 = -\lambda \frac{F_{i-\frac{1}{2}}^-}{(s_i^{n+1} + a_l'(\zeta_i^{n+\frac{1}{2}}))} \frac{\delta_i}{2(c_{l+1}^n - c_l^n)}. \end{aligned}$$

From the property of the limiter it is easy to see that

$$0 \leq \frac{\delta_{i+1}}{2(c_{l+1}^n - c_l^n)} \leq 1 \quad (30)$$

which in turn implies

$$C_{i-\frac{1}{2}}^n, D_{i+\frac{1}{2}}^n \geq 0 \quad \forall i. \quad (31)$$

Now we prove the maximum principle for c_l ($l = 1, 2$) by considering the following cases.

Case1: Suppose that $c_{l_i}^n$ lies between $c_{l_{i-1}}^n$ and $c_{l_{i+1}}^n$ then

$$c_{l_i}^n = \theta c_{l_{i-1}}^n + (1 - \theta) c_{l_{i+1}}^n \quad \text{for some } \theta \in [0, 1]$$

and

$$\begin{aligned} c_{l_i}^n - c_{l_{i-1}}^n &= (1 - \theta) (c_{l_{i+1}}^n - c_{l_{i-1}}^n) \\ c_{l_{i+1}}^n - c_{l_i}^n &= \theta (c_{l_{i+1}}^n - c_{l_{i-1}}^n). \end{aligned}$$

Now from (29) we write

$$\begin{aligned}
c_{l_i}^{n+1} &= (1 - \theta)(c_{l_{i+1}}^n - c_{l_{i-1}}^n) - C_{i-\frac{1}{2}}^n(1 - \theta)(c_{l_{i+1}}^n - c_{l_{i-1}}^n) \\
&\quad + D_{i+\frac{1}{2}}^n \theta(c_{l_{i+1}}^n - c_{l_{i-1}}^n) \\
&= \lambda_1 c_{l_{i-1}}^n + \lambda_2 c_{l_{i+1}}^n,
\end{aligned} \tag{32}$$

where

$$\begin{aligned}
\lambda_1 &= \theta(1 - D_{i+\frac{1}{2}}^n) + C_{i-\frac{1}{2}}^n(1 - \theta) \\
\lambda_2 &= (1 - \theta)(1 - C_{i-\frac{1}{2}}^n) + \theta D_{i+\frac{1}{2}}^n.
\end{aligned}$$

Note that $\lambda_1 + \lambda_2 = 1$, under the CFL condition $\lambda M \leq \frac{1}{2}$ we have $C_{i-\frac{1}{2}}^n, D_{i+\frac{1}{2}}^n \leq 1$ which gives $\lambda_1, \lambda_2 \geq 0$. Hence from (32) the maximum principle (a) follows.

Case2: Suppose $c_{l_i}^n$ does not lies between $c_{l_{i-1}}^n$ and $c_{l_{i+1}}^n$, then we have $\delta_i = 0$. i.e.,

$$C_{i-\frac{1}{2}}^n = \alpha_{i-\frac{1}{2}}^3 \text{ and } D_{i+\frac{1}{2}}^n = \alpha_{i+\frac{1}{2}}^2$$

The equation (29) can be rewritten as

$$c_{l_i}^{n+1} = (1 - C_{i-\frac{1}{2}}^n - D_{i+\frac{1}{2}}^n)c_{l_i}^n + C_{i-\frac{1}{2}}^n c_{l_{i-1}}^n + D_{i+\frac{1}{2}}^n c_{l_{i+1}}^n.$$

Note that

$$C_{i-\frac{1}{2}}^n + D_{i+\frac{1}{2}}^n \leq 1 \text{ under the CFL condition } \lambda M \leq \frac{1}{2}.$$

This proves the maximum principle(a).

To prove the TVD property, consider

$$\begin{aligned}
C_{i+\frac{1}{2}}^n + D_{i+\frac{1}{2}}^n &= \lambda \frac{F_{i+\frac{3}{2}}^+}{(s_i^{n+1} + a_l'(\zeta_i^{n+\frac{1}{2}}))2(c_{l_{i+1}}^n - c_{l_i}^n)} \delta_{i+1} \\
&\quad + \lambda \frac{F_{i+\frac{1}{2}}^+}{(s_i^{n+1} + a_l'(\zeta_i^{n+\frac{1}{2}}))} (1 - \frac{\delta_i}{2(c_{l_{i+1}}^n - c_{l_i}^n)}) \\
&\quad - \lambda \frac{F_{i+\frac{1}{2}}^-}{(s_i^{n+1} + a_l'(\zeta_i^{n+\frac{1}{2}}))} (1 - \frac{\delta_{i+1}}{2(c_{l_{i+1}}^n - c_{l_i}^n)}) \\
&\quad - \lambda \frac{F_{i-\frac{1}{2}}^-}{(s_i^{n+1} + a_l'(\zeta_i^{n+\frac{1}{2}}))} \frac{\delta_i}{2(c_{l_{i+1}}^n - c_{l_i}^n)} \\
&\leq \lambda M \left(\frac{\delta_{i+1}}{2(c_{l_{i+1}}^n - c_{l_i}^n)} + 1 - \frac{\delta_i}{2(c_{l_{i+1}}^n - c_{l_i}^n)} \right. \\
&\quad \left. + 1 - \frac{\delta_{i+1}}{2(c_{l_{i+1}}^n - c_{l_i}^n)} + \frac{\delta_i}{2(c_{l_{i+1}}^n - c_{l_i}^n)} \right) \\
&= 2\lambda M \leq 1,
\end{aligned} \tag{34}$$

under the CFL condition $\lambda M \leq \frac{1}{2}$. From (31) and (34) the TVD property(b) follows from the Harten's lemma. ■

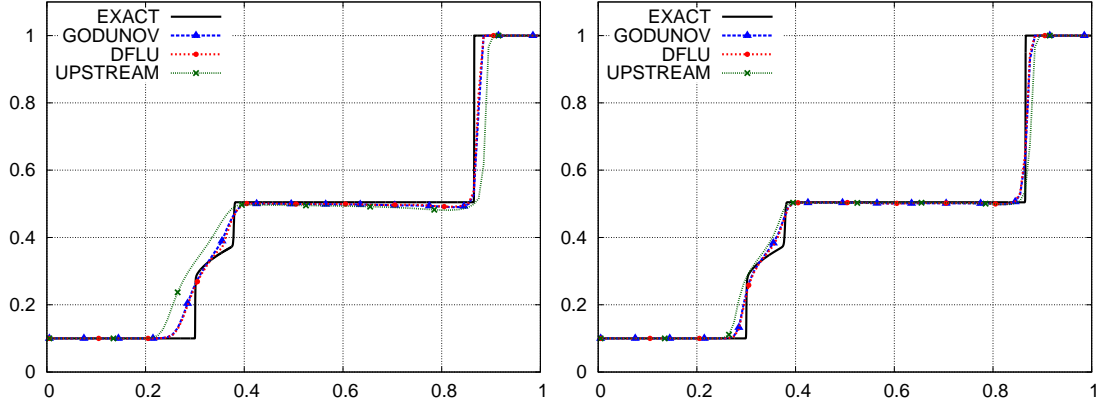


Figure 8: Saturation s for first order scheme (left), high order scheme (right) at time $t = 1$, mesh size $h = \frac{1}{100}$.

Remark: Note that saturation s need not be of total variation bounded because of $f = f(s, c)$ and $c = c(x, t)$ is discontinuous (see [1]). The singular mapping technique as in [3] to prove the convergence of $s_{i,j}^n$ looks very difficult to apply. However by using the method of compensated compactness, Kalrsen, Mishra, Risebro [28] showed the convergence of approximated solution in the case of a triangular system. By using their results in the case of a single component polymer ($m = 1$) under suitable assumptions, in [4] convergence analysis of the saturation is studied.

2.9 Numerical results

Here we have chosen the flux function for the above system of equations (7) with $v = 0.2$, $K \equiv 1$, $\lambda_w = \frac{s^2}{0.5+c_1+c_2}$, $\lambda_o = (1-s)^2$, $\rho_w g = 2$ and $\rho_o g = 1$. The adsorption term is given by $a_l(c_l) = 1 + 0.5c_l$ ($l = 1, 2$). In the numerical experiment the initial data is chosen so that the flux function F is allowed to change the sign, equivalently eigenvalues λ^l ($l = 1, 2$) of the system (7) allowed to change the sign. For this purpose the initial data is chosen as

$$(s(x, 0), c_1(x, 0), c_2(x, 0)) = \begin{cases} (0.1, 1, 0.6) & \text{if } x < 0.4 \\ (1.0, 0, 0) & \text{if } x > 0.4. \end{cases}$$

Numerical experiments are done for DFLU flux, Upstream mobility flux and compared with Godunov flux. In these experiments data are chosen so that DFLU flux differ from Godunov flux. The performance of the DFLU flux is as good as the Godunov flux. High order accurate schemes corresponding to DFLU and Godunov are constructed by introducing slope limiter in space variable and a strong stability preserving Runge-Kutta scheme in the time variable, a comparison with first order scheme is shown in Fig.8,9. For first order and high order scheme it clearly shows that the DFLU flux is as good as the Godunov flux. Note that Godunov flux requires the solution of the Riemann problem of a system where as DFLU flux requires the solution of the Riemann problem of a scalar equation. Fig.10,11,12 shows that numerical solution computed by DFLU is as good as Godunov and converges faster than Upstream mobility scheme.

For high order scheme the L^1 error, order of accuracy α for DFLU, Godunov and Upstream mobility schemes are given in the table 1. The order of accuracy α is calculated as follows:

$$e_1 = \|s - s_{h_1}\|_{L^1} \text{ with } h_1 = h, \quad e_2 = \|s - s_{h_2}\|_{L^1} \text{ with } h_2 = h/2, \quad \alpha = \frac{\ln(e_1/e_2)}{\ln 2}.$$

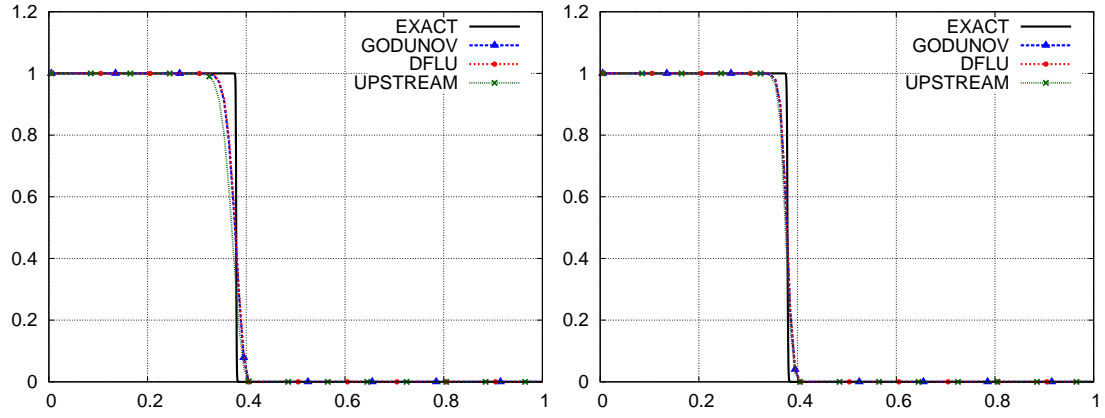


Figure 9: Concentration c_1 for first order scheme (left), high order scheme (right) at time $t = 1$ (right), mesh size $h = \frac{1}{100}$.

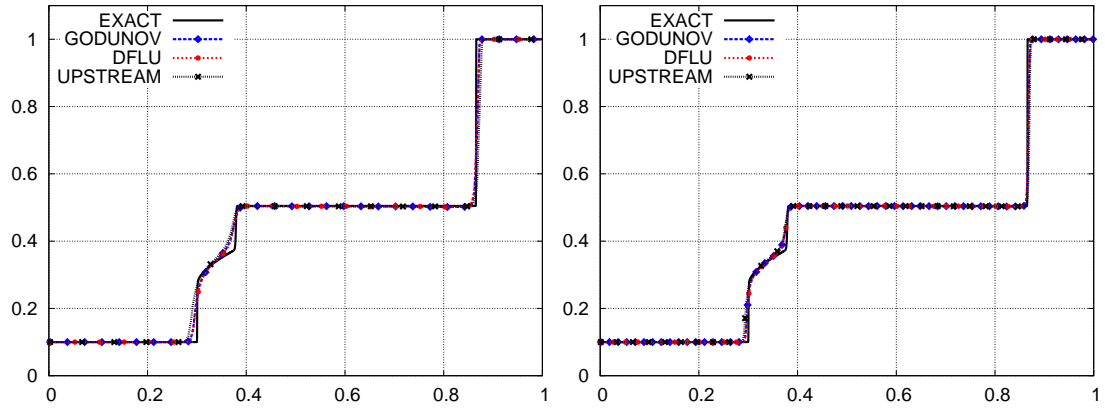


Figure 10: Saturation s at time $t = 1$ with mesh size $h = \frac{1}{200}$ (left) and $h = \frac{1}{400}$ (right), with high order accuracy.

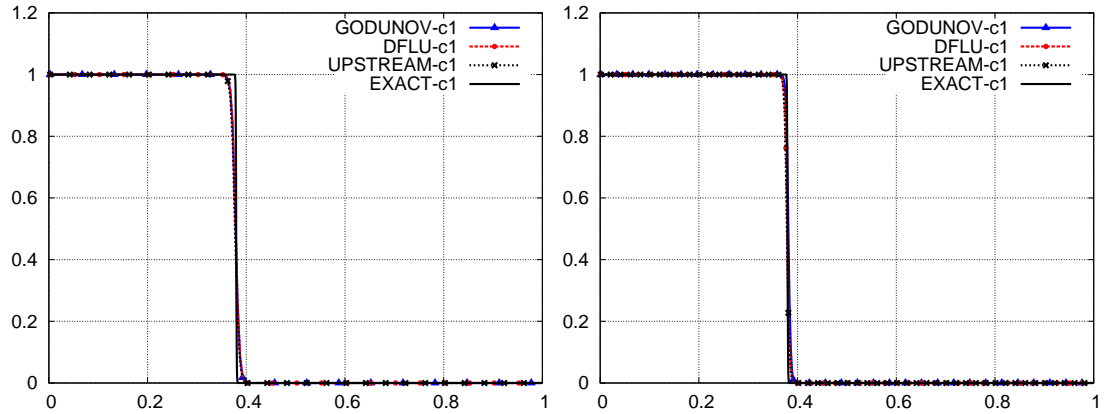


Figure 11: Concentration c_1 at time $t = 1$ with mesh size $h = \frac{1}{200}$ (left) and $h = \frac{1}{400}$ (right), with high order accuracy.

h	DFLU $\ s - s^h\ _{L^1}$	α	GODUNOV $\ s - s^h\ _{L^1}$	α	UPSTREAM $\ s - s^h\ _{L^1}$	α
1/50	4.2336×10^{-2}		4.8839×10^{-2}		6.3189×10^{-2}	
1/100	2.4366×10^{-2}	0.7970	2.7735×10^{-2}	0.8163	3.6055×10^{-2}	0.8095
1/200	1.3605×10^{-2}	0.8407	1.5268×10^{-2}	0.8612	1.9805×10^{-2}	0.8643
1/400	6.2334×10^{-3}	1.1260	6.9589×10^{-3}	1.133	9.2108×10^{-3}	1.1045
1/800	2.2233×10^{-3}	1.4873	2.4398×10^{-3}	1.5121	3.3674×10^{-3}	1.4517

h	DFLU $\ c_1 - c_1^h\ _{L^1}$	α	GODUNOV $\ c_1 - c_1^h\ _{L^1}$	α	UPSTREAM $\ c_1 - c_1^h\ _{L^1}$	α
1/50	3.3257×10^{-2}		3.9971×10^{-2}		5.0529×10^{-2}	
1/100	2.2303×10^{-2}	0.5764	2.5938×10^{-2}	0.6239	3.4946×10^{-2}	0.5319
1/200	1.2304×10^{-2}	0.8582	1.4014×10^{-2}	0.8881	1.874×10^{-2}	0.899
1/400	4.8878×10^{-3}	1.3318	5.4714×10^{-3}	1.3569	7.9071×10^{-3}	1.2449
1/800	1.6586×10^{-3}	1.5592	1.8413×10^{-3}	1.5712	2.8197×10^{-3}	1.4876

h	DFLU $\ c_2 - c_2^h\ _{L^1}$	α	GODUNOV $\ c_2 - c_2^h\ _{L^1}$	α	UPSTREAM $\ c_2 - c_2^h\ _{L^1}$	α
1/50	1.9954×10^{-2}		2.3983×10^{-2}		3.0318×10^{-2}	
1/100	1.3382×10^{-2}	0.5764	1.5563×10^{-2}	0.6239	2.0968×10^{-2}	0.5319
1/200	7.3821×10^{-3}	0.8581	8.4086×10^{-3}	0.8881	1.1244×10^{-2}	0.899
1/400	2.9327×10^{-3}	1.3318	3.2829×10^{-3}	1.3569	4.7455×10^{-3}	1.2445
1/800	9.9518×10^{-4}	1.5592	1.10479×10^{-3}	1.5712	1.6924×10^{-3}	1.4875

Table 1: L^1 error for saturation s and concentrations c_1 and c_2 .

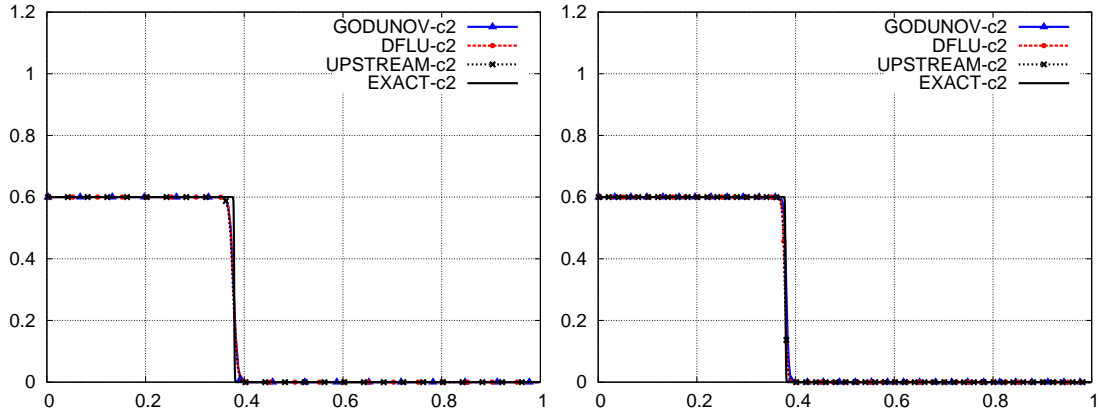


Figure 12: Concentration c_2 at time $t = 1$ with mesh size $h = \frac{1}{200}$ (left) and $h = \frac{1}{400}$ (right), with high order accuracy.

Note that as $h \rightarrow 0$, α in DFLU is better than α in Upstream and more close to α in GODUNOV. Here the exact solutions $s, c = (c_1, c_2)$ are computed from Godunov scheme for very small values of h and Δt with $\frac{\Delta t}{h} M = 0.5$.

3 2-D model

In this section we are extending the numerical schemes explained in § 2 for one dimension to a multi dimensional space. For simplicity we explain only in two dimensions and higher dimension can be handled in a similar way. In dimension two the equation (1) can be rewritten as

$$\begin{aligned} s_t + \frac{\partial F_1}{\partial x_1}(s, c, x) + \frac{\partial F_2}{\partial x_2}(s, c, x) &= 0 \\ (sc_1 + a_1(c_1))_t + \frac{\partial c_1 F_1}{\partial x_1}(s, c, x) + \frac{\partial c_1 F_2}{\partial x_2}(s, c, x) &= 0 \\ (sc_2 + a_2(c_2))_t + \frac{\partial c_2 F_1}{\partial x_1}(s, c, x) + \frac{\partial c_2 F_2}{\partial x_2}(s, c, x) &= 0 \end{aligned} \quad (35)$$

where $(x, t) \in \Omega \times (0, \infty)$, $x = (x_1, x_2)$ and the flux $F_1, F_2 : [0, 1] \times [0, c_0]^2 \times \Omega \rightarrow \mathbb{R}$ are given by

$$F_1(s, c, x) = v_1(x)f(s, c), \quad f(s, c) = \frac{\lambda_w(s, c)}{\lambda_w(s, c) + \lambda_o(s)} \quad (36)$$

$$F_2(s, c, x) = [v_2(x) - (\rho_w - \rho_o)g\lambda_o(s, c)K(x)]f(s, c) \quad (37)$$

To compute F_1 and F_2 we need the velocity component $v = (v_1, v_2)$. This velocity (pressure) is governed by the incompressibility of the flow:

$$\nabla \cdot v = 0 \quad \text{in } \Omega \quad (38)$$

with some suitable boundary condition for velocity (pressure) on $\partial\Omega$ as explained in § 1.

Basic numerical approach for finite volume method is outlined in the following algorithm:

1. Set time step $n = 0$ and initialize $s^0, c^0 = (c_1^0, c_2^0)$.
2. Assume s^n and $c^n = (c_1^n, c_2^n)$ are known at $t = t_n$.
3. Solve for the pressure p^n from (4) and (5).
4. Compute velocity v^n from (4).
5. Chose time step Δt^n so that CFL condition is satisfied see §3.5 .
6. Update saturation and concentration at $t = t_{n+1}$ level by

$$\begin{aligned} s^{n+1} &= s^n - \Delta t^n \nabla \cdot (F(s^n, c^n, v^n)) \\ s^{n+1}c_1^{n+1} + a_1(c_1^{n+1}) &= s^n c_1^n + a_1(c_1^n) - \Delta t^n \nabla \cdot (c_1^n F(s^n, c^n, v^n)) \\ s^{n+1}c_2^{n+1} + a_1(c_2^{n+1}) &= s^n c_2^n + a_2(c_2^{n+1}) - \Delta t^n \nabla \cdot (c_2^n F(s^n, c^n, v^n)) \end{aligned}$$

7. Set $n = n + 1$ and Go to step 2.

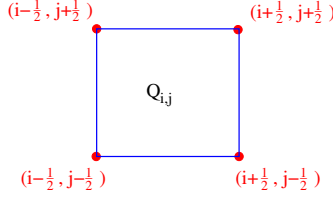


Figure 13: Definition of cell $Q_{i,j}$ by grid points

3.1 Discretization of the domain $\Omega = [0, 1] \times [0, 1]$

Consider the Cartesian grid obtained by taking the cross product of the one-dimensional partitions $\{x_i, i = 1, \dots, n_x\}$ and $\{y_j, j = 1, \dots, n_y\}$ with $x_1 = y_1 = 0$ and $x_{n_x} = y_{n_y} = 1$. We also introduce one layer of grid points on all four sides of Ω which will be referred to as ghost points. Thus the grid point indices range over $0 \leq i \leq n_x + 1$ and $0 \leq j \leq n_y + 1$. The grid defines the cell $Q_{i,j} = [x_{i-\frac{1}{2}}, x_{i+\frac{1}{2}}] \times [y_{j-\frac{1}{2}}, y_{j+\frac{1}{2}}]$, see Fig.13, for $0 \leq i \leq n_x$ and $0 \leq j \leq n_y$. The number of true cells where the solution is supposed to be computed in the domain Ω is $n_c = (n_x - 1) \times (n_y - 1)$ (excluding the ghost cells).

3.2 Numerical approximation for the pressure

Define $\mu := (\lambda_w + \lambda_o)K$ and $\theta := (\lambda_w \rho_w + \lambda_o \rho_o)gK$. Integrating equation (5) over cell $Q_{i,j}$ and using the divergence theorem, we obtain the finite volume approximation

$$(v_{i+\frac{1}{2},j} - v_{i-\frac{1}{2},j})\Delta y + (v_{i,j+\frac{1}{2}} - v_{i,j-\frac{1}{2}})\Delta x = 0 \quad (39)$$

where the velocity at the cell face is given by

$$v_{i+\frac{1}{2},j} = -\mu \frac{\partial p}{\partial x} \Big|_{i+\frac{1}{2},j}, \quad v_{i,j+\frac{1}{2}} = -(\mu \frac{\partial p}{\partial y} + \theta) \Big|_{i,j+\frac{1}{2}}$$

We approximate these as follows:

- Along the x-direction

$$\begin{aligned} p_{i+1,j} - p_{i,j} &= \int_{x_i}^{x_{i+1}} \mu \frac{\partial p}{\partial x} \frac{1}{\mu} dx \approx \mu \frac{\partial p}{\partial x} \Big|_{i+\frac{1}{2},j} \int_{x_i}^{x_{i+1}} \frac{1}{\mu} dx \\ &\approx \mu \frac{\partial p}{\partial x} \Big|_{i+\frac{1}{2},j} \frac{1}{2} \left(\frac{1}{\mu_{i,j}} + \frac{1}{\mu_{i+1,j}} \right) \Delta x \end{aligned}$$

This leads to the following approximation for the velocity flux

$$v_{i+\frac{1}{2},j} = -\bar{\mu}_{i+\frac{1}{2},j} \frac{p_{i+1,j} - p_{i,j}}{\Delta x}, \quad \frac{1}{\bar{\mu}_{i+\frac{1}{2},j}} = \frac{1}{2} \left(\frac{1}{\mu_{i,j}} + \frac{1}{\mu_{i+1,j}} \right) \quad (40)$$

- Along the y-direction

$$\begin{aligned} p_{i,j+1} - p_{i,j} &= \int_{y_j}^{y_{j+1}} \frac{1}{\mu} \left[\mu \frac{\partial p}{\partial y} + \theta - \theta \right] dy \approx -v_{i,j+\frac{1}{2}} \int_{y_j}^{y_{j+1}} \frac{1}{\mu} - \int_{y_j}^{y_{j+1}} \frac{\theta}{\mu} \\ &\approx -v_{i,j+\frac{1}{2}} \frac{\Delta y}{2} \left(\frac{1}{\mu_{i,j}} + \frac{1}{\mu_{i,j+1}} \right) - \frac{\Delta y}{2} \left(\frac{\theta_{i,j}}{\mu_{i,j}} + \frac{\theta_{i,j+1}}{\mu_{i,j+1}} \right). \end{aligned}$$

Hence we get the approximation

$$v_{i,j+\frac{1}{2}} = -\bar{\mu}_{i,j+\frac{1}{2}} \frac{p_{i,j+1} - p_{i,j}}{\Delta y} - \bar{\theta}_{i,j+\frac{1}{2}} \quad (41)$$

where

$$\frac{1}{\bar{\mu}_{i,j+\frac{1}{2}}} := \frac{1}{2} \left(\frac{1}{\mu_{i,j}} + \frac{1}{\mu_{i,j+1}} \right), \quad \bar{\theta}_{i,j+\frac{1}{2}} := \frac{\bar{\mu}_{i,j+\frac{1}{2}}}{2} \left(\frac{\theta_{i,j}}{\mu_{i,j}} + \frac{\theta_{i,j+1}}{\mu_{i,j+1}} \right). \quad (42)$$

The velocity on the inlet boundary is computed as

$$v_{\frac{1}{2},j} = -\bar{\mu}_{\frac{1}{2},j} \frac{p_{1,j} - p_I}{\Delta x}, \quad \frac{1}{\bar{\mu}_{\frac{1}{2},j}} = \frac{1}{2} \left(\frac{1}{\mu_{0,j}} + \frac{1}{\mu_{1,j}} \right) \quad (43)$$

with similar expressions for the other inlet/outlet parts of the boundary. On the rest of the boundary, the normal velocity is zero which is equivalent to saying that flux is zero. The system of equations (39) for the pressure can be put in the form

$$Ap = b \quad (44)$$

where $A \in \mathbb{R}^{n_c \times n_c}$ and $b \in \mathbb{R}^{n_c}$. This matrix equation is solved using conjugate the gradient method.

3.3 Finite volume scheme

By integrating equations in (1) over the cell $Q_{i,j}$, we obtain the following finite volume approximations

$$s_{i,j}^{n+1} = s_{i,j}^n - \frac{\Delta t}{\Delta x \Delta y} \left\{ [F_{i+\frac{1}{2},j}^n - F_{i-\frac{1}{2},j}^n] \Delta y + [F_{i,j+\frac{1}{2}}^n - F_{i,j-\frac{1}{2}}^n] \Delta x \right\}, \quad (45)$$

$$s_{i,j}^{n+1} c_{1,i,j}^{n+1} + a_1(c_{1,i,j}^{n+1}) = s_{i,j}^n c_{1,i,j}^n + a_1(c_{1,i,j}^n) - \frac{\Delta t}{\Delta x \Delta y} \left\{ [(c_1 F)_{i+\frac{1}{2},j}^n - (c_1 F)_{i-\frac{1}{2},j}^n] \Delta y + [(c_1 F)_{i,j+\frac{1}{2}}^n - (c_1 F)_{i,j-\frac{1}{2}}^n] \Delta x \right\}, \quad (46)$$

$$s_{i,j}^{n+1} c_{2,i,j}^{n+1} + a_2(c_{2,i,j}^{n+1}) = s_{i,j}^n c_{2,i,j}^n + a_2(c_{2,i,j}^n) - \frac{\Delta t}{\Delta x \Delta y} \left\{ [(c_2 F)_{i+\frac{1}{2},j}^n - (c_2 F)_{i-\frac{1}{2},j}^n] \Delta y + [(c_2 F)_{i,j+\frac{1}{2}}^n - (c_2 F)_{i,j-\frac{1}{2}}^n] \Delta x \right\}. \quad (47)$$

Here we introduce the DFLU numerical flux for two dimensional finite volume scheme by using the idea explained in §2. The corresponding numerical fluxes are given by

$$F_{i+\frac{1}{2},j}^n = \max\{F_1(\max(s_{i,j}^n, (\theta_{F_1}^n)_{i,j}), c_{i,j}^n, K_{i,j}), F_1(\min(s_{i+1,j}^n, (\theta_{F_1}^n)_{i+1,j}), c_{i+1,j}^n, K_{i+1,j})\}$$

$$F_{i,j+\frac{1}{2}}^n = \max\{F_2(\max(s_{i,j}^n, (\theta_{F_2}^n)_{i,j}), c_{i,j}^n, K_{i,j}), F_2(\min(s_{i,j+1}^n, (\theta_{F_2}^n)_{i,j+1}), c_{i,j+1}^n, K_{i,j+1})\}$$

where $c_{i,j}^n = (c_{1,i,j}^n, c_{2,i,j}^n)$ and

$$(\theta_{F_1}^n)_{i,j} = \operatorname{argmin} F_1(., c_{i,j}^n, K_{i,j}) \text{ and } (\theta_{F_2}^n)_{i,j} = \operatorname{argmin} F_2(., c_{i,j}^n, K_{i,j})$$

$$(c_l F)_{i+\frac{1}{2},j}^n = \begin{cases} c_{l,i,j} F_{i+\frac{1}{2},j}^n & \text{if } F_{i+\frac{1}{2},j}^n > 0 \\ c_{l,i+1,j} F_{i+\frac{1}{2},j}^n & \text{if } F_{i+\frac{1}{2},j}^n \leq 0 \end{cases} \quad l = 1, 2.$$

3.4 High-order scheme

In order to develop the second order scheme, we follow the method of lines approach in which space and time discretization are performed separately. In the first step, spatial discretization using piecewise linear reconstruction is made which leads to a system of ODE which can be written as

$$\frac{dU}{dt} + R(U) = 0, \quad U = \begin{bmatrix} s \\ sc_1 + a_1(c_1) \\ sc_2 + a_2(c_2) \end{bmatrix} \quad (48)$$

where

$$R(U)_{i,j} = \frac{1}{\Delta x \Delta y} \begin{bmatrix} [F_{i+\frac{1}{2},j} - F_{i-\frac{1}{2},j}] \Delta y + [F_{i,j+\frac{1}{2}} - F_{i,j-\frac{1}{2}}] \Delta x \\ [G_{1i+\frac{1}{2},j} - G_{1i-\frac{1}{2},j}] \Delta y + [G_{1i,j+\frac{1}{2}} - G_{1i,j-\frac{1}{2}}] \Delta x \\ [G_{2i+\frac{1}{2},j} - G_{2i-\frac{1}{2},j}] \Delta y + [G_{2i,j+\frac{1}{2}} - G_{2i,j-\frac{1}{2}}] \Delta x \end{bmatrix} \quad (49)$$

The high order accurate fluxes are given by

$$F_{i+\frac{1}{2},j} = \bar{F}(s_{i+\frac{1}{2},j}^L, s_{i+\frac{1}{2},j}^R, c_{1i+\frac{1}{2},j}^L, c_{2i+\frac{1}{2},j}^L, c_{1i+\frac{1}{2},j}^R, c_{2i+\frac{1}{2},j}^R, v_{i+\frac{1}{2},j}, K_{i,j}, K_{i+1,j})$$

$$G_{li+\frac{1}{2},j} = \begin{cases} c_{li+\frac{1}{2},j}^L F_{i+\frac{1}{2},j} & \text{if } F_{i+\frac{1}{2},j} > 0 \\ c_{li+\frac{1}{2},j}^R F_{i+\frac{1}{2},j} & \text{if } F_{i+\frac{1}{2},j} \leq 0 \end{cases} \quad l = 1, 2, \quad (50)$$

and similar expression for $F_{i,j+\frac{1}{2}}$. The quantities with superscripts L and R denote the reconstructed values of the variables to the left and right of the cell face. For any quantity u , we can define the reconstruction in x -direction as follows:

$$u_{i+\frac{1}{2},j}^L = u_{i,j} + \frac{1}{2} \delta_{i,j}^x, \quad u_{i+\frac{1}{2},j}^R = u_{i+1,j} - \frac{1}{2} \delta_{i+1,j}^x \quad (51)$$

where

$$\delta_{i,j}^x = \min \left(\theta(u_{i,j} - u_{i-1,j}), \frac{1}{2}(u_{i+1,j} - u_{i-1,j}), \theta(u_{i+1,j} - u_{i,j}) \right), \quad \theta \in [1, 2]. \quad (52)$$

Similarly in the y -direction we can define $u_{i,j+\frac{1}{2}}^L$ and $u_{i,j+\frac{1}{2}}^R$.

3.5 Stability results

Let us write

$$\bar{s}^n = (\bar{s}_i^n)_{i=1}^8 = (s_{i-\frac{1}{2},j}^{n,L}, s_{i-\frac{1}{2},j}^{n,R}, s_{i+\frac{1}{2},j}^{n,L}, s_{i+\frac{1}{2},j}^{n,R}, s_{i,j-\frac{1}{2}}^{n,L}, s_{i,j-\frac{1}{2}}^{n,R}, s_{i,j+\frac{1}{2}}^{n,L}, s_{i,j+\frac{1}{2}}^{n,R})$$

$$\bar{c}^n = (\bar{c}_i^n)_{i=1}^{16} = (c_{i-\frac{1}{2},j}^{n,L}, c_{i-\frac{1}{2},j}^{n,R}, c_{i+\frac{1}{2},j}^{n,L}, c_{i+\frac{1}{2},j}^{n,R}, c_{i,j-\frac{1}{2}}^{n,L}, c_{i,j-\frac{1}{2}}^{n,R}, c_{i,j+\frac{1}{2}}^{n,L}, c_{i,j+\frac{1}{2}}^{n,R})_{l=1,2}$$

The updated value of the saturation (45) can be written as

$$s_{i,j}^{n+1} = H(\bar{s}^n, \bar{c}^n, v_{i\pm\frac{1}{2},j}, v_{i,j\pm\frac{1}{2}}, K_{i\pm 1,j}, K_{i,j}, K_{i,j\pm 1}).$$

Where H is Lipschitz continuous in saturation and concentration with the property

$$H(\mathbf{0}, v_{i\pm\frac{1}{2},j}, v_{i,j\pm\frac{1}{2}}, K_{i\pm 1,j}, K_{i,j}, K_{i,j\pm 1}) = 0$$

$$H(\mathbf{1}, v_{i\pm\frac{1}{2},j}, v_{i,j\pm\frac{1}{2}}, K_{i\pm 1,j}, K_{i,j}, K_{i,j\pm 1}) = 1.$$

Since the slope limiter preserves the average value of the solution in each cell, we can express this as

$$s_{i,j}^{n+1} = \frac{s_{i+\frac{1}{2},j}^{n,L} + s_{i-\frac{1}{2},j}^{n,R}}{4} + \frac{s_{i,j+\frac{1}{2}}^{n,L} + s_{i,j-\frac{1}{2}}^{n,R}}{4} - \frac{\Delta t}{\Delta x}(F_{i+\frac{1}{2},j}^n - F_{i-\frac{1}{2},j}^n) - \frac{\Delta t}{\Delta y}(F_{i,j+\frac{1}{2}}^n - F_{i,j-\frac{1}{2}}^n). \quad (53)$$

If we differentiate H with respect to its variables \bar{s}_i^n we can observe that $\frac{\partial}{\partial \bar{s}_i^n} H \geq 0$ provided

$$\lambda^x \left| \frac{\partial}{\partial \bar{s}_i^n} F_{i\pm\frac{1}{2},j}^n \right|, \lambda^y \left| \frac{\partial}{\partial \bar{s}_i^n} F_{i,j\pm\frac{1}{2}}^n \right| \leq \frac{1}{4}. \quad (54)$$

Let

$$M = \sup_s \left\{ \frac{\partial F_1}{\partial s}, \frac{\partial F_2}{\partial s}, \frac{F_1}{s + h_l}, \frac{F_2}{s + h_l} \right\},$$

then the condition (54) reduces to,

$$\max\{\lambda^x M, \lambda^y M\} \leq \frac{1}{4}, \text{ where } \lambda^x = \frac{\Delta t}{\Delta x}, \lambda^y = \frac{\Delta t}{\Delta y}. \quad (55)$$

This shows that H is monotone in each of its variable. Using these facts we have the following lemmas.

Lemma 3.1 *Let $s_0 \in [0, 1]$ be the initial data and let $\{s_{i,j}^n\}$ be the corresponding solution calculated by the finite volume scheme (45) using DFLU flux along with slope limiter. If the CFL given in (55) holds then*

$$0 \leq s_{i,j}^n \leq 1 \quad \forall, i, j \text{ and } n. \quad (56)$$

Proof: From the property of slope limiter we can observe that whenever $0 \leq s_{i,j}^n \leq 1$ then the reconstructed values satisfies

$$0 \leq s_{i\pm\frac{1}{2},j}^{n,L,R}, s_{i,j\pm\frac{1}{2}}^{n,L,R} \leq 1 \quad \forall, i, j \text{ and } n.$$

Using this property and the monotonicity of the H , we get

$$\begin{aligned} 0 &= H(\mathbf{0}, \bar{c}^n, v_{i\pm\frac{1}{2},j}, v_{i,j\pm\frac{1}{2}}, K_{i\pm 1,j}, K_{i,j}, K_{i,j\pm 1}) \\ &\leq H(\bar{s}^n, \bar{c}^n, v_{i\pm\frac{1}{2},j}, v_{i,j\pm\frac{1}{2}}, K_{i\pm 1,j}, K_{i,j}, K_{i,j\pm 1}) = s_{i,j}^{n+1} \\ &\leq H(\mathbf{1}, \bar{c}^n, v_{i\pm\frac{1}{2},j}, v_{i,j\pm\frac{1}{2}}, K_{i\pm 1,j}, K_{i,j}, K_{i,j\pm 1}) = 1 \end{aligned}$$

This proves that

$$0 \leq s_{i,j}^{n+1} \leq 1 \quad \forall, i, j.$$

■

Now we prove the lemma that gives the maximum principle for the concentration.

Lemma 3.2 *Let $\{c_{1,i,j}^n\}, \{c_{2,i,j}^n\}$ be the solution calculated by the finite volume scheme (46) and (47) by using DFLU flux with slope limiter. Under the CFL condition (55) concentration $c = (c_1, c_2)$ satisfies the following maximum principle*

$$\begin{aligned} (a) \quad \min\{c_{l,i,j}^n, c_{l,i\pm 1,j}^n, c_{l,i,j\pm 1}^n\} &\leq c_{l,i,j}^{n+1} \leq \max\{c_{l,i,j}^n, c_{l,i\pm 1,j}^n, c_{l,i,j\pm 1}^n\}, \\ &\forall n \in \mathbb{Z}^+, i \in \mathbb{Z}, l = 1, 2. \end{aligned}$$

Proof: We can express the high order numerical fluxes $G_{l_{i+\frac{1}{2},j}}, G_{l_{i,j+\frac{1}{2}}}$ ($l = 1, 2$) in the finite volume scheme (46) and (47) as

$$\begin{aligned} G_{l_{i+\frac{1}{2},j}} &= c_{l_{i+\frac{1}{2},j}}^{nL} F_{i+\frac{1}{2},j}^+ + c_{l_{i+\frac{1}{2},j}}^{nR} F_{i+\frac{1}{2},j}^- \\ G_{l_{i,j+\frac{1}{2}}} &= c_{l_{i,j+\frac{1}{2}}}^{nL} F_{i,j+\frac{1}{2}}^+ + c_{l_{i,j+\frac{1}{2}}}^{nR} F_{i,j+\frac{1}{2}}^-, \end{aligned}$$

where

$$\begin{aligned} F_{i+\frac{1}{2},j}^+ &= \max\{F_{i+\frac{1}{2},j}, 0\}, \quad F_{i+\frac{1}{2},j}^- = \min\{F_{i+\frac{1}{2},j}, 0\} \\ F_{i,j+\frac{1}{2}}^+ &= \max\{F_{i,j+\frac{1}{2}}, 0\}, \quad F_{i,j+\frac{1}{2}}^- = \min\{F_{i,j+\frac{1}{2}}, 0\}. \end{aligned}$$

We write the scheme (46) and (47) ($l = 1, 2$) as

$$\begin{aligned} s_{i,j}^{n+1} c_{i,j}^{n+1} + a_l(c_{i,j}^{n+1}) - s_{i,j}^n c_{i,j}^n - a_l(c_{i,j}^n) + \lambda^x (c_{l_{i+\frac{1}{2},j}}^L F_{i+\frac{1}{2},j}^+ + c_{l_{i+\frac{1}{2},j}}^R F_{i+\frac{1}{2},j}^- - c_{l_{i-\frac{1}{2},j}}^L F_{i-\frac{1}{2},j}^+ - c_{l_{i-\frac{1}{2},j}}^R F_{i-\frac{1}{2},j}^-) \\ + \lambda^y (c_{l_{i,j+\frac{1}{2}}}^L F_{i,j+\frac{1}{2}}^+ + c_{l_{i,j+\frac{1}{2}}}^R F_{i,j+\frac{1}{2}}^- - c_{l_{i,j-\frac{1}{2}}}^L F_{i,j-\frac{1}{2}}^+ - c_{l_{i,j-\frac{1}{2}}}^R F_{i,j-\frac{1}{2}}^-) = 0. \end{aligned}$$

By adding and subtracting the terms $s_{i,j}^{n+1} c_{i,j}^n$ we get

$$\begin{aligned} (s_{i,j}^{n+1} + a'_l(\zeta_i^{n+\frac{1}{2}}))(c_{i,j}^{n+1} - c_{i,j}^n) + c_{i,j}^n (s_{i,j}^{n+1} - s_{i,j}^n) \\ + \lambda^x (c_{l_{i+\frac{1}{2},j}}^{nL} F_{i+\frac{1}{2},j}^+ + c_{l_{i+\frac{1}{2},j}}^{nR} F_{i+\frac{1}{2},j}^- - c_{l_{i-\frac{1}{2},j}}^{nL} F_{i-\frac{1}{2},j}^+ - c_{l_{i-\frac{1}{2},j}}^{nR} F_{i-\frac{1}{2},j}^-) \\ + \lambda^y (c_{l_{i,j+\frac{1}{2}}}^{nL} F_{i,j+\frac{1}{2}}^+ + c_{l_{i,j+\frac{1}{2}}}^{nR} F_{i,j+\frac{1}{2}}^- - c_{l_{i,j-\frac{1}{2}}}^{nL} F_{i,j-\frac{1}{2}}^+ - c_{l_{i,j-\frac{1}{2}}}^{nR} F_{i,j-\frac{1}{2}}^-) = 0. \end{aligned}$$

where $a_l(c_{i,j}^{n+1}) - a_l(c_{i,j}^n) = a'_l(\zeta_{i,j}^{n+\frac{1}{2}})(c_{i,j}^{n+1} - c_{i,j}^n)$, for some $\zeta_{i,j}^{n+\frac{1}{2}}$ between $c_{i,j}^{n+1}$ and $c_{i,j}^n$. Replacing $s_{i,j}^{n+1} - s_{i,j}^n$ by $-\lambda^x (F_{i+\frac{1}{2},j} - F_{i-\frac{1}{2},j}) - \lambda^y (F_{i,j+\frac{1}{2}} - F_{i,j-\frac{1}{2}})$ and splitting $F_{i\pm\frac{1}{2},j}$ by $F_{i\pm\frac{1}{2},j}^+ + F_{i\pm\frac{1}{2},j}^-$ (similarly for $F_{i,j\pm\frac{1}{2}}$) and by rearranging the terms we have

$$\begin{aligned} (s_{i,j}^{n+1} + a'_l(\zeta_{i,j}^{n+\frac{1}{2}}))(c_{i,j}^{n+1} - c_{i,j}^n) + \lambda^x F_{i+\frac{1}{2},j}^+ (c_{l_{i+\frac{1}{2},j}}^{nL} - c_{i,j}^n) + \lambda^x F_{i+\frac{1}{2},j}^- (c_{l_{i+\frac{1}{2},j}}^{nR} - c_{i,j}^n) \\ + \lambda^x F_{i-\frac{1}{2},j}^+ (c_{i,j}^n - c_{l_{i-\frac{1}{2},j}}^{nL}) + \lambda^x F_{i-\frac{1}{2},j}^- (c_{i,j}^n - c_{l_{i-\frac{1}{2},j}}^{nR}) \\ + \lambda^y F_{i,j+\frac{1}{2}}^+ (c_{i,j+\frac{1}{2}}^{nL} - c_{i,j}^n) + \lambda^y F_{i,j+\frac{1}{2}}^- (c_{i,j+\frac{1}{2}}^{nR} - c_{i,j}^n) \\ + \lambda^y F_{i,j-\frac{1}{2}}^+ (c_{i,j}^n - c_{l_{i,j-\frac{1}{2}}}^{nL}) + \lambda^y F_{i,j-\frac{1}{2}}^- (c_{i,j}^n - c_{l_{i,j-\frac{1}{2}}}^{nR}) = 0. \end{aligned}$$

Note that

$$c_{l_{i+\frac{1}{2},j}}^{nL} = c_{i,j}^n + \frac{\delta_{i,j}^x}{2}, \quad c_{l_{i-\frac{1}{2},j}}^{nR} = c_{i,j}^n - \frac{\delta_{i,j}^x}{2}, \quad c_{l_{i,j+\frac{1}{2}}}^{nL} = c_{i,j}^n + \frac{\delta_{i,j}^y}{2}, \quad c_{l_{i,j-\frac{1}{2}}}^{nR} = c_{i,j}^n - \frac{\delta_{i,j}^y}{2}$$

and $\delta_{i,j}^x$ and $\delta_{i,j}^y$ are the slope limiter given by

$$\begin{aligned} \delta_{i,j}^x &= \min\text{mod} \left(\theta(c_{i,j}^n - c_{i-1,j}^n), \frac{1}{2}(c_{i+1,j}^n - c_{i-1,j}^n), \theta(c_{i+1,j}^n - c_{i,j}^n) \right), \\ \delta_{i,j}^y &= \min\text{mod} \left(\theta(c_{i,j}^n - c_{i,j-1}^n), \frac{1}{2}(c_{i,j+1}^n - c_{i,j-1}^n), \theta(c_{i,j+1}^n - c_{i,j}^n) \right). \end{aligned}$$

After substituting the values of $c_{l_{i,j} \pm \frac{1}{2},j}^{nL}$, $c_{l_{i,j} \pm \frac{1}{2},j}^{nR}$, $c_{l_{i,j} \pm \frac{1}{2},j}^{nL}$, $c_{l_{i,j} \pm \frac{1}{2},j}^{nR}$ the above equation becomes

$$\begin{aligned}
c_{l_{i,j}}^{n+1} = & c_{l_{i,j}}^n - \lambda^x \frac{F_{i+\frac{1}{2},j}^+}{(s_{i,j}^{n+1} + a'_l(\zeta_{i,j}^{n+\frac{1}{2}}))(c_{l_{i,j}}^n - c_{l_{i-1,j}}^n)} \frac{\delta_{i,j}^x}{2} (c_{l_{i,j}}^n - c_{l_{i-1,j}}^n) \\
& - \lambda^x \frac{F_{i+\frac{1}{2},j}^-}{(s_{i,j}^{n+1} + a'_l(\zeta_{i,j}^{n+\frac{1}{2}}))} (1 - \frac{\delta_{i+1,j}^x}{2(c_{l_{i+1,j}}^n - c_{l_{i,j}}^n)}) (c_{l_{i+1,j}}^n - c_{l_{i,j}}^n) \\
& - \lambda^x \frac{F_{i-\frac{1}{2},j}^+}{(s_{i,j}^{n+1} + a'_l(\zeta_{i,j}^{n+\frac{1}{2}}))} (1 - \frac{\delta_{i-1,j}^x}{2(c_{l_{i,j}}^n - c_{l_{i-1,j}}^n)}) (c_{l_{i,j}}^n - c_{l_{i-1,j}}^n) \\
& - \lambda^x \frac{F_{i-\frac{1}{2},j}^-}{(s_{i,j}^{n+1} + a'_l(\zeta_{i,j}^{n+\frac{1}{2}}))(c_{l_{i+1,j}}^n - c_{l_{i,j}}^n)} \frac{\delta_{i,j}^x}{2} (c_{l_{i+1,j}}^n - c_{l_{i,j}}^n) \\
& - \lambda^y \frac{F_{i,j+\frac{1}{2}}^+}{(s_{i,j}^{n+1} + a'_l(\zeta_{i,j}^{n+\frac{1}{2}}))(c_{l_{i,j}}^n - c_{l_{i,j-1}}^n)} \frac{\delta_{i,j}^y}{2} (c_{l_{i,j}}^n - c_{l_{i,j-1}}^n) \\
& - \lambda^y \frac{F_{i,j+\frac{1}{2}}^-}{(s_{i,j}^{n+1} + a'_l(\zeta_{i,j}^{n+\frac{1}{2}}))} (1 - \frac{\delta_{i,j+1}^y}{2(c_{l_{i,j+1}}^n - c_{l_{i,j}}^n)}) (c_{l_{i,j+1}}^n - c_{l_{i,j}}^n) \\
& - \lambda^y \frac{F_{i,j-\frac{1}{2}}^+}{(s_{i,j}^{n+1} + a'_l(\zeta_{i,j}^{n+\frac{1}{2}}))} (1 - \frac{\delta_{i,j-1}^y}{2(c_{l_{i,j}}^n - c_{l_{i,j-1}}^n)}) (c_{l_{i,j}}^n - c_{l_{i,j-1}}^n) \\
& - \lambda^y \frac{F_{i,j-\frac{1}{2}}^-}{(s_{i,j}^{n+1} + a'_l(\zeta_{i,j}^{n+\frac{1}{2}}))(c_{l_{i,j+1}}^n - c_{l_{i,j}}^n)} \frac{\delta_{i,j}^y}{2} (c_{l_{i,j+1}}^n - c_{l_{i,j}}^n),
\end{aligned}$$

Now we write it as

$$\begin{aligned}
c_{l_{i,j}}^{n+1} = & c_{l_{i,j}}^n - \alpha_{i-\frac{1}{2},j}^1 (c_{l_{i,j}}^n - c_{l_{i-1,j}}^n) + \alpha_{i+\frac{1}{2},j}^2 (c_{l_{i+1,j}}^n - c_{l_{i,j}}^n) - \alpha_{i-\frac{1}{2},j}^3 (c_{l_{i,j}}^n - c_{l_{i-1,j}}^n) \\
& + \alpha_{i+\frac{1}{2},j}^4 (c_{l_{i+1,j}}^n - c_{l_{i,j}}^n) - \alpha_{i,j-\frac{1}{2}}^1 (c_{l_{i,j}}^n - c_{l_{i,j-1}}^n) + \alpha_{i,j+\frac{1}{2}}^2 (c_{l_{i,j+1}}^n - c_{l_{i,j}}^n) \\
& - \alpha_{i,j-\frac{1}{2}}^3 (c_{l_{i,j}}^n - c_{l_{i,j-1}}^n) + \alpha_{i,j+\frac{1}{2}}^4 (c_{l_{i,j+1}}^n - c_{l_{i,j}}^n) \\
= & c_{l_{i,j}}^n - C_{i-\frac{1}{2},j}^n (c_{l_{i,j}}^n - c_{l_{i-1,j}}^n) + D_{i+\frac{1}{2},j}^n (c_{l_{i+1,j}}^n - c_{l_{i,j}}^n) \\
& - C_{i,j-\frac{1}{2}}^n (c_{l_{i,j}}^n - c_{l_{i,j-1}}^n) + D_{i,j+\frac{1}{2}}^n (c_{l_{i,j+1}}^n - c_{l_{i,j}}^n), \tag{57}
\end{aligned}$$

where

$$\begin{aligned}
C_{i-\frac{1}{2},j}^n &= \alpha_{i-\frac{1}{2},j}^1 + \alpha_{i-\frac{1}{2},j}^3, & D_{i+\frac{1}{2},j}^n &= \alpha_{i+\frac{1}{2},j}^2 + \alpha_{i+\frac{1}{2},j}^4 \\
C_{i,j-\frac{1}{2}}^n &= \alpha_{i,j-\frac{1}{2}}^1 + \alpha_{i,j-\frac{1}{2}}^3, & D_{i,j+\frac{1}{2}}^n &= \alpha_{i,j+\frac{1}{2}}^2 + \alpha_{i,j+\frac{1}{2}}^4
\end{aligned}$$

and

$$\begin{aligned}
\alpha_{i-\frac{1}{2},j}^1 &= \lambda^x \frac{F_{i+\frac{1}{2},j}^+}{(s_{i,j}^{n+1} + a'_l(\zeta_{i,j}^{n+\frac{1}{2}}))(c_{l_{i,j}}^n - c_{l_{i-1,j}}^n)} \frac{\delta_{i,j}^x}{2}, \\
\alpha_{i+\frac{1}{2},j}^2 &= -\lambda^x \frac{F_{i+\frac{1}{2},j}^-}{(s_{i,j}^{n+1} + a'_l(\zeta_{i,j}^{n+\frac{1}{2}}))} \left(1 - \frac{\delta_{i+1,j}^x}{2(c_{l_{i+1,j}}^n - c_{l_{i,j}}^n)}\right), \\
\alpha_{i-\frac{1}{2},j}^3 &= \lambda^x \frac{F_{i-\frac{1}{2},j}^+}{(s_{i,j}^{n+1} + a'_l(\zeta_{i,j}^{n+\frac{1}{2}}))} \left(1 - \frac{\delta_{i-1,j}^x}{2(c_{l_{i,j}}^n - c_{l_{i-1,j}}^n)}\right), \\
\alpha_{i+\frac{1}{2},j}^4 &= -\lambda^x \frac{F_{i-\frac{1}{2},j}^-}{(s_{i,j}^{n+1} + a'_l(\zeta_{i,j}^{n+\frac{1}{2}}))(c_{l_{i+1,j}}^n - c_{l_{i,j}}^n)} \frac{\delta_{i,j}^x}{2}, \\
\alpha_{i,j-\frac{1}{2}}^1 &= \lambda^y \frac{F_{i,j+\frac{1}{2}}^+}{(s_{i,j}^{n+1} + a'_l(\zeta_{i,j}^{n+\frac{1}{2}}))(c_{l_{i,j}}^n - c_{l_{i,j-1}}^n)} \frac{\delta_{i,j}^y}{2}, \\
\alpha_{i,j+\frac{1}{2}}^2 &= -\lambda^y \frac{F_{i,j+\frac{1}{2}}^-}{(s_{i,j}^{n+1} + a'_l(\zeta_{i,j}^{n+\frac{1}{2}}))} \left(1 - \frac{\delta_{i,j+1}^y}{2(c_{l_{i,j+1}}^n - c_{l_{i,j}}^n)}\right), \\
\alpha_{i,j-\frac{1}{2}}^3 &= \lambda^y \frac{F_{i,j-\frac{1}{2}}^+}{(s_{i,j}^{n+1} + a'_l(\zeta_{i,j}^{n+\frac{1}{2}}))} \left(1 - \frac{\delta_{i,j-1}^y}{2(c_{l_{i,j}}^n - c_{l_{i,j-1}}^n)}\right), \\
\alpha_{i,j+\frac{1}{2}}^4 &= -\lambda^y \frac{F_{i,j-\frac{1}{2}}^-}{(s_{i,j}^{n+1} + a'_l(\zeta_{i,j}^{n+\frac{1}{2}}))(c_{l_{i,j+1}}^n - c_{l_{i,j}}^n)} \frac{\delta_{i,j}^y}{2}.
\end{aligned}$$

From the property of the limiter it is easy to see that

$$0 \leq \frac{\delta_{i+1,j}^x}{2(c_{l_{i+1,j}}^n - c_{l_{i,j}}^n)}, \quad \frac{\delta_{i+1,j}^y}{2(c_{l_{i,j+1}}^n - c_{l_{i,j}}^n)} \leq 1,$$

which in turn implies that

$$C_{i-\frac{1}{2},j}^n, C_{i,j-\frac{1}{2}}^n, D_{i+\frac{1}{2},j}^n, D_{i,j+\frac{1}{2}}^n \geq 0.$$

Now we prove the maximum principle through following cases.

Case 1: Suppose that

- (a) $c_{l_{i,j}}^n$ lies between $c_{l_{i-1,j}}^n$, and $c_{l_{i+1,j}}^n$ and
- (b) $c_{l_{i,j}}^n$ lies between $c_{l_{i,j+1}}^n$, and $c_{l_{i,j-1}}^n$, then

$$c_{l_{i,j}}^n = \theta^x c_{l_{i-1,j}}^n + (1 - \theta^x) c_{l_{i+1,j}}^n \quad \text{for some } \theta^x \in [0, 1] \text{ and} \quad (58)$$

$$c_{l_{i,j}}^n = \theta^y c_{l_{i,j-1}}^n + (1 - \theta^y) c_{l_{i,j+1}}^n \quad \text{for some } \theta^y \in [0, 1]. \quad (59)$$

Now

$$\begin{aligned}
c_{l_{i,j}}^n - c_{l_{i-1,j}}^n &= (1 - \theta^x)(c_{l_{i+1,j}}^n - c_{l_{i-1,j}}^n), \\
c_{l_{i+1,j}}^n - c_{l_{i,j}}^n &= \theta^x(c_{l_{i+1,j}}^n - c_{l_{i-1,j}}^n), \\
c_{l_{i,j}}^n - c_{l_{i,j-1}}^n &= (1 - \theta^y)(c_{l_{i,j+1}}^n - c_{l_{i,j-1}}^n), \\
c_{l_{i,j+1}}^n - c_{l_{i,j}}^n &= \theta^y(c_{l_{i,j+1}}^n - c_{l_{i,j-1}}^n).
\end{aligned}$$

By writing $c_{l,i,j}^n$ as $\frac{1}{2}(c_{l,i,j}^n + c_{l,i,j}^n)$ and substituting the values from (58) and (59) the equation (57) becomes

$$\begin{aligned} c_{l,i,j}^{n+1} &= \frac{1}{2}(\theta^x c_{l,i-1,j}^n + (1 - \theta^x) c_{l,i+1,j}^n) - C_{i-\frac{1}{2},j}^n (1 - \theta^x)(c_{l,i+1,j}^n - c_{l,i-1,j}^n) \\ &\quad + D_{i+\frac{1}{2},j}^n \theta^x (c_{l,i+1,j}^n - c_{l,i-1,j}^n) + \frac{1}{2}(\theta^y c_{l,i,j-1}^n + (1 - \theta^y) c_{l,i,j+1}^n) \\ &\quad - C_{i,j-\frac{1}{2}}^n (1 - \theta^y)(c_{l,i,j+1}^n - c_{l,i,j-1}^n) + D_{i,j+\frac{1}{2}}^n \theta^y (c_{l,i,j+1}^n - c_{l,i,j-1}^n), \\ &= \lambda_1 c_{l,i-1,j}^n + \lambda_2 c_{l,i+1,j}^n + \lambda_3 c_{l,i,j-1}^n + \lambda_4 c_{l,i,j+1}^n, \end{aligned} \quad (60)$$

where

$$\begin{aligned} \lambda_1 &= (1 - \theta^x) C_{i-\frac{1}{2},j}^n + \theta^x (\frac{1}{2} - D_{i+\frac{1}{2},j}^n), \\ \lambda_2 &= (1 - \theta^x) (\frac{1}{2} - C_{i-\frac{1}{2},j}^n) + \theta^x D_{i+\frac{1}{2},j}^n, \\ \lambda_3 &= (1 - \theta^y) C_{i,j-\frac{1}{2}}^n + \theta^y (\frac{1}{2} - D_{i,j+\frac{1}{2}}^n), \\ \lambda_4 &= (1 - \theta^y) (\frac{1}{2} - C_{i,j-\frac{1}{2}}^n) + \theta^y D_{i,j+\frac{1}{2}}^n. \end{aligned}$$

Note that $\lambda_1 + \lambda_2 + \lambda_3 + \lambda_4 = 1$ and with the CFL condition (55) we have

$$C_{i-\frac{1}{2},j}^n, C_{i,j-\frac{1}{2}}^n, D_{i+\frac{1}{2},j}^n, D_{i,j+\frac{1}{2}}^n \leq \frac{1}{2}$$

which gives $\lambda_1, \lambda_2, \lambda_3, \lambda_4 \geq 0$. Hence from (60) the maximum principle follows.

Case2: Suppose that

- (a) $c_{l,i,j}^n$ does not lie between $c_{l,i-1,j}^n$ and $c_{l,i+1,j}^n$ and
- (b) $c_{l,i,j}^n$ does not lie between $c_{l,i,j+1}^n$ and $c_{l,i,j-1}^n$, then we have $\delta_{i,j}^x = \delta_{i,j}^y = 0$. i.e.,

$$C_{i-\frac{1}{2},j}^n = \alpha_{i-\frac{1}{2},j}^3, D_{i+\frac{1}{2},j}^n = \alpha_{i+\frac{1}{2},j}^2, C_{i,j-\frac{1}{2}}^n = \alpha_{i,j-\frac{1}{2}}^3 \text{ and } D_{i,j+\frac{1}{2}}^n = \alpha_{i,j+\frac{1}{2}}^2.$$

The equation (57) can be written as

$$\begin{aligned} c_{l,i,j}^{n+1} &= (1 - C_{i-\frac{1}{2},j}^n - D_{i+\frac{1}{2},j}^n - C_{i,j-\frac{1}{2}}^n - D_{i,j+\frac{1}{2}}^n) c_{l,i,j}^n \\ &\quad + C_{i-\frac{1}{2},j}^n c_{l,i-1,j}^n + D_{i+\frac{1}{2},j}^n c_{l,i+1,j}^n + C_{i,j-\frac{1}{2}}^n c_{l,i,j-1}^n + D_{i,j+\frac{1}{2}}^n c_{l,i,j+1}^n. \end{aligned}$$

Note that

$$C_{i-\frac{1}{2},j}^n + D_{i+\frac{1}{2},j}^n + C_{i,j-\frac{1}{2}}^n + D_{i,j+\frac{1}{2}}^n \leq 1, \quad \text{under the CFL condition (55).}$$

This proves the maximum principle. Other cases can be handled in a similar way and the maximum principle can be shown.

3.6 Numerical experiments

For numerical simulation we have chosen an example of the quarter five-spot problem in the domain $[0, 1] \times [0, 1]$. To show the effect of gravity numerical experiments are performed in the presence of gravity as well as in the absence of gravity. Also to study the polymer flooding effect numerical experiments are performed for various concentration of the polymers. The behavior of water saturation is studied when the polymers are injected with different concentrations. The flux function $F = (F_1, F_2)$ takes the same form as in equation (36) and (37) with

$$\lambda_w = \frac{s^2}{\mu_w(c_1, c_2)}, \lambda_o = (1 - s)^2, \rho_w g = 2 \text{ and } \rho_o g = 1, a_l(c_l) = 1 + 0.5c_l \ (l = 1, 2)$$

and velocity v across the grid point is calculated by using (39).

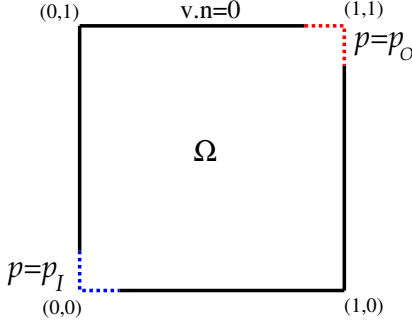


Figure 14: Reservoir domain and boundary conditions

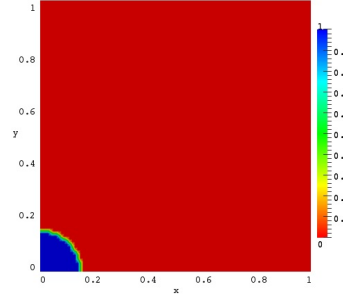


Figure 15: Pumping water through the inlet boundary

3.7 Initial and boundary conditions

The simulations are performed in a computational domain $\Omega = [0, 1] \times [0, 1]$ for $t \in [0, 1]$. The initial condition is $s(x, 0) = 0$, i.e. In the inlet part of the boundary we pump water with a pressure $p = p_I$ and we keep the outlet part of the boundary with a pressure $p = p_O$ ($p_I > p_O$), on the remaining part of the boundary normal velocity is set to zero. The initial inlet saturation is shown in Fig.14 and 15

3.8 Permeability of the porous media

We consider a heterogeneous porous medium with an absolute permeability $K(x)$. In order to illustrate the robustness of the proposed numerical scheme we consider the two model porous media. The first test case corresponds to a heterogeneous medium with a continuous random permeability given by

$$K(x) = \min\{\max\{\sum_{i=0}^N \Phi_i(x), 0.5\}, 1.5\} \quad (61)$$

and

$$\Phi_i(x) = \exp(-(\frac{|x - x_i|}{0.05})^2)$$

where x_i are N randomly chosen locations inside the domain. Here we have taken $N = 100$. The second test case corresponds to a heavily heterogeneous medium with hard rocks and the permeability is given by choosing N random locations x_i and

$$K(x) = \begin{cases} 0.01 & \text{if } x \in B(x_i, 0.0015) \text{ for some } i \in \{1, 2, \dots, N\} \\ 1 & \text{eslewhere} \end{cases} \quad (62)$$

The permeability fields for these two test cases are shown in Fig.16

Experiment 1: Simulations in this experiment was performed using the spatial permeability distribution given in (61), shown in Fig.16(a). The viscosity of water is given by $\mu_w(c_1, c_2) = 0.5 + c_1 + c_2$. We inject water through the inlet boundary with an inlet pressure $p_I = 8$ and inlet concentration $c_1 = 0$ and $c_2 = 0$. This is the case of without polymer. As expected it produces fingering effects, consequently when the water front touches the outlet boundary, a large amount of oil is stuck in the remaining portion of the domain, which reduces the efficiency of oil-recovery, this is shown in Fig.17(a). To avoid this instability polymer is dissolved with water and injected through the inlet wall. In the presence of polymer

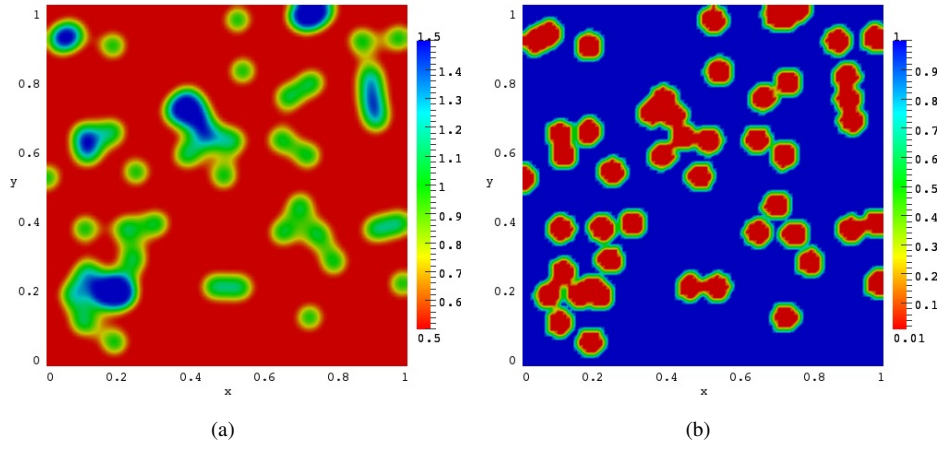


Figure 16: (a) Permeability fields for (61), (b) Permeability fields for (62) .

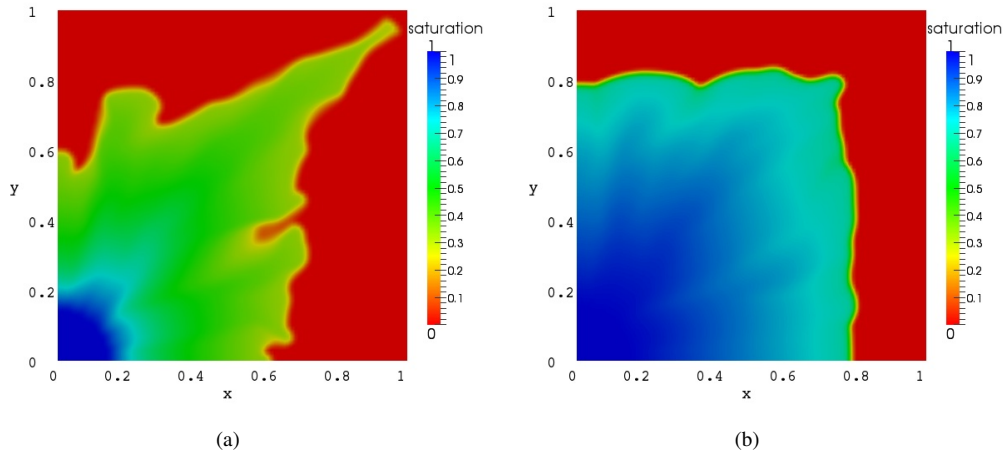


Figure 17: (a) Saturation s in the absence of a polymer (b) Saturation s in the presence of a polymer.

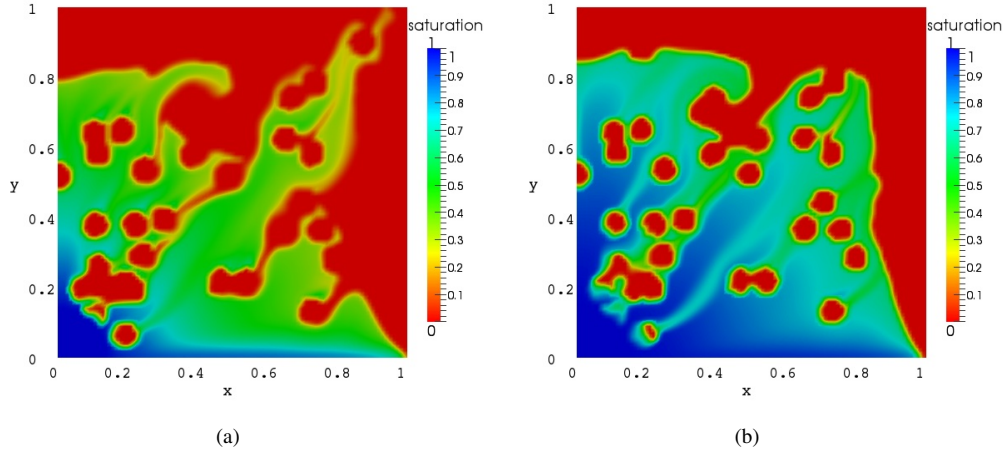


Figure 18: (a) Saturation s in experiment 2, in the absence of polymer (b) Saturation s in experiment 2, in the presence of polymer.

say $c_1 = 7$ and $c_2 = 0$ the fingering instability almost disappears and the amount of oil produced at the recovery well (outlet boundary) is increased. This is shown in Fig.17(b).

Experiment 2: The permeability field is chosen as in expression (62) with the presence of gravity, shown in Fig.16(b). Which corresponds to a heavily heterogeneous media with hard rocks. Here we have taken viscosity of water as $\mu_w(c_1, c_2) = 0.5 + c_1 + c_2$. The result obtained in Fig.18(a) corresponds to the saturation profile with the inlet concentration $c_1 = 0$ and $c_2 = 0$. The result obtained in Fig.18(b) corresponds to the saturation profile with inlet concentration $c_1 = 5$ and $c_2 = 3$. A consistent behavior of the saturation profile shows that our proposed scheme works well with varying spatial discontinuity in the media.

Experiment 3: This experiment is mainly to study the effect of gravity in saturation profile. This experiment is performed using spatial permeability distributions given in (62), shown in Fig.16(b). Viscosity takes the form $\mu_w(c_1, c_2) = 0.5 + c_1 + c_2$. We chose the inlet concentrations as $c_1 = 7$ and $c_2 = 0$. The expression involving gravity term is considered along the y direction (see eqn (37)). The resulting figures are shown in Fig.19(a) with the absence of gravity and Fig.19(b) with presence of gravity. Observe that presence of gravity significantly effects the saturation profile.

Experiment 4: This experiment is to study the effect of adding more than one polymer with different concentrations. In this model we have taken $\mu_w(c_1, c_2) = 0.5 + \sqrt{c_1} + \sqrt{c_2}$ and permeability field is chosen as in (62). Figure 20(a) corresponds to the case with concentrations $c_1 = 49, c_2 = 0$. In figure 20(b) we have taken the concentrations to be $c_1 = 25, c_2 = 24$. Observe that the total amount $(c_1 + c_2)$ of injected concentrations in both the case are the same. But in the second case by adding two concentrations the sweeping profile of water saturation is improved considerably. This is reflected in fig 20(b). It is clear from this fact that by adding multiple polymers and by taking a suitable viscosity $\mu_w(c_1, c_2)$ it may be possible to maximize the oil-recovery.

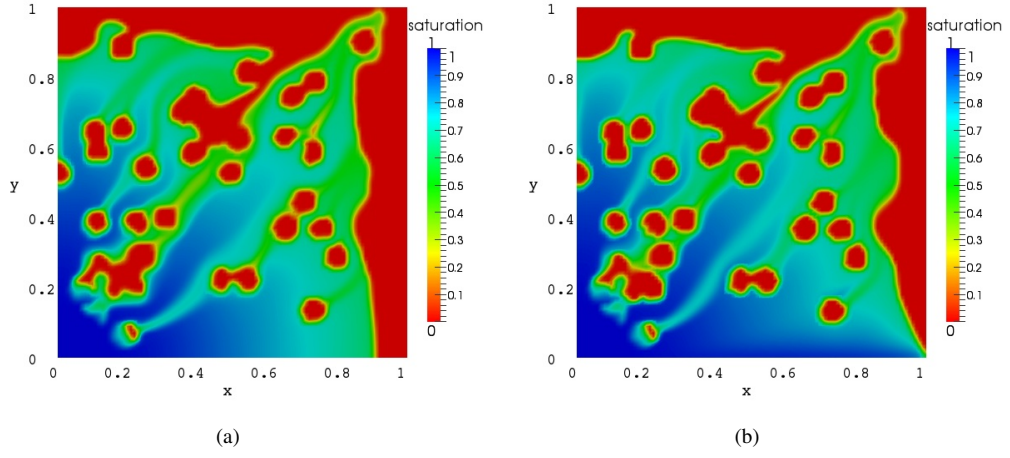


Figure 19: (a) With out the effect of gravity (b) With the effect of gravity

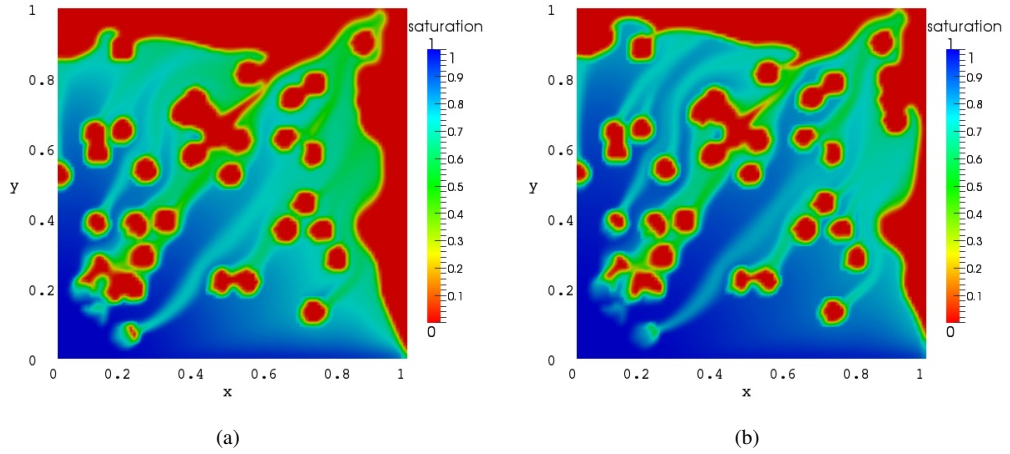


Figure 20: (a) Single component (b) Multicomponent

4 Conclusion.

A high resolution finite volume scheme is developed to study the two-phase flow in porous media by using the idea of discontinuous flux. The idea of discontinuous flux helps to reduce the system to an uncoupled scalar equation with discontinuous coefficients. Discontinuous flux uses the solution of the Riemann problem of the scalar equation where as the Godunov flux needs solution of the Riemann problem of the coupled system which is difficult to construct especially in the presence of gravity, heterogeneity and multiple components. The results obtained from the idea of discontinuous flux agrees well with the results obtained from the Godunov flux. The two-phase flow is studied in the presence as well as in the absence of gravity. It is shown that the presence of gravity affects the saturation profile. Also the efficiency of

the numerical method is demonstrated by performing numerical simulations corresponding to two-phase flow in heterogeneous media.

References

- [1] Adimurthi, Rajib Dutta, S.S. Ghoshal and G.D.Veerappa Gowda, *Existence and nonexistence of TV bounds for scalar conservation laws with discontinuous flux*, Comm.Pure Appl.Math. LXIV(2011) 0084-0115.
- [2] Adimurthi and G. D Veerappa Gowda, *Conservation laws with discontinuous flux*, J.Math.Kyoto.Univ.43(1)(2003)27-70.
- [3] Adimurthi,J. Jaffré and G. D. Veerappa Gowda, *Godunov-type methods for conservation laws with a flux function discontinuous in space*, SINUM,**42** (2004), pp. 179-208.
- [4] Adimurthi, G. D. V. Gowda, and J. Jaffre, *The DFLU flux for systems of conservation laws*, To appear in J. Comput. Appl. Math.
- [5] Aziz K, Settari A, *Petroleum reservoir simulation*, London, Applied science publishers Ltd, 1979.
- [6] Bear J, *Dynamics of fluids in porous media*, American Elsevier, 1972. Bejan A and Nield DA, *Convection in porous media*, New York, Springer, 2006.
- [7] Branets, Larisa V.; Ghai, Sartaj S.; Lyons, Stephen L.; Wu, Xiao-Hui, *Challenges and technologies in reservoir modeling*, Commun. Comput. Phys 6 (2009), no. 1, pp. 1–23.
- [8] Brenier, Yann; Jaffré, Jérôme, *Upstream differencing for multiphase flow in reservoir simulation*, SIAM J. Numer. Anal **28** (1991), no. 3, pp. 685–696.
- [9] R. Bürger K.H. Karlsen, and J.D. Towers, *An Engquist-Osher-type scheme for conservation laws with discontinuous flux adapted to flux connections*, SIAM J. Numer. Anal. 47 (2009), no. 3, 1684–1712.
- [10] R. Burger, K.H. Karlsen, N.H. Risebro and J.D. Towers, *Well-posedness in BVt and convergence of a difference scheme for continuous sedimentation in ideal clarifier-thickener units*, Numer. Math. 97 (1) (2004) 25–65
- [11] G. Chavent, G. Cohen and J. Jaffré, *A finite element simulator for incompressible two-phase flow*, Transport in Porous Media, 2 (1987), pp. 465–478.
- [12] Prabir Daripa, James Glimm, Brent Lindquist and Oliver McBryan, *Polymer floods: a case study of nonlinear wave analysis and of instability control in tertiary oil-recovery*, Siam J.Appl. Math **48**.(1988), pp.353-373.
- [13] S . Diehl, *Conservation laws with application to continuous sedimentation*, Doctoral Dissertation, Lund University, Lund Sweden, pp. 1-21.
- [14] S. Diehl, *On scalar conservation law with point source and discontinuous flux functions*, SIAM J. Math. Anal, 26 (1995), pp. 1425-1451.
- [15] Lister S, Djilali N, *Two-phase transport in porous gas diffusion electrodes*, in: Faghri M, Sunden B, editors. Southampton(UK): WIT press. 2005.
- [16] R. E. Ewing, editor, *The mathematics of reservoir simulation*, SIAM, Philadelphia, 1983.

- [17] R. Eymard, C. Guichard, R. Herbin, R. Masson *Gradient schemes for two-phase flow in heterogeneous porous media and Richards equation*, submitted to ZAMM - Journal of Applied Mathematics and Mechanics 2012.
- [18] T. Gimse and N. H. Risebro, *Solution of the Cauchy problem for a conservation law with a discontinuous flux function*, SIAM J. Math. Anal., 23 (1992), pp. 635–648.
- [19] J. Glimm, D. Marchesin and O. McBryan, *Unstable fingers in two phase flow*,. Comm. Pure and Appl. Math, 34 (1981), pp. 53-75.
- [20] Gottlieb Sigal, *On high order strong stability preserving Runge-Kutta and multi step time discretizations*, J. Sci. Comput. 25 (2005), no. 1-2, 105–128. (Reviewer: Martin Hermann) 65L06 (65L20 65M20).
- [21] Sigal Gottlieb And Chi-Wang Shu, *Total variation diminishing Runge-Kutta schemes*, Math.Comp,(1998), pp.73-85.
- [22] J. Jaffre, *Flux calculation at the interface between two rock types for two-phase flow in porous media*, Transp. Porous Media, 21 (1995), pp. 195–207.
- [23] T. Johansen, A. Tveito and R. Winther, *A Riemann solver for a two-phase multicomponent process*, SIAM J. Sci. Stat. Comput, Vol.10, No. 5,(1989), pp. 846-879.
- [24] T. Johansen, R. Winther, *The solution of the Riemann problem for a hyperbolic system of conservation laws modeling polymer flooding*, SIAM J. Math. Anal., 19 (1988), pp. 541-566.
- [25] T. Johansen, R. Winther, *The Riemann problem for multicomponent polymer flooding*, SIAM J. Math. Anal, 20, No. 4,(1989), pp. 908-929
- [26] E.F. Kaasschieter, *Solving the Buckley-Leverett equation with gravity in a heterogeneous porous medium*, Computational Geosciences, 3 (1999), pp. 23–48.
- [27] K.H. Karlsen, Lie, K.A. and N.H. Risebro, *A fast marching method for reservoir simulation*, Computational Geosciences. 4 (2000), no. 2, 185–206.
- [28] K.H. Karlsen, S. Mishra and N.H. Risebro, *Convergence of finite volume schemes for triangular systems of conservation laws*, Numer. Math. 111(4) (2009) 559-589.
- [29] K.H. Karlsen, S. Mishra and N. H. Risebro, *Semi-Godunov schemes for multiphase flows in porous media*, App.Num.Math.,59(9)(2009)2322-2336.
- [30] K.H. Karlsen, N.H. Risebro, J.D. Towers, *L^1 stability for entrolpy solutions of nonlinear degenerate parabolic convection-diffusion equations with discontinuous coefficients*, Skr. K. Nor. Vidensk, Selsk. 3 (2003) 1–49.
- [31] Klingenberg, Christian; Risebro and Nils Henrik, *Stability of a resonant system of conservation laws modeling polymer flow with gravitation*, J. Differential Equations. 170 (2001), no. 2, pp. 344–380.
- [32] H.P. Langtangen, A. Tveito, and R. Winther, *Instability of Buckley-Leverett flow in heterogeneous media*, Transp. Porous Media, 9(1992), pp. 165–185.
- [33] P.D. Lax, *Hyperbolic systems of conservation laws II*, Pure Appl. Math., 10 (1957), pp. 537-566.
- [34] Mishra, Siddhartha; Jaffré, Jérôme, *On the upstream mobility scheme for two-phase flow in porous media*, Comput. Geosci **14** (2010), no. 1, pp. 105–124.

- [35] D.W. Peaceman, *Fundamentals of Numeical Reservoir Simulation*, Elsevier, Amsterdam, 1977.
- [36] J.Smoller, *Shock Waves and Reaction-Diffusion Equations*, Springer-Verlag, Berlin, New York 1982.
- [37] A. Tveito, R. Winther, *Existence, uniqueness, and continuous dependence for a system of hyperbolic conservation laws modeling polymer flooding*, SIAM J. Math. Anal. 22 (1991), no. 4.